Many-to-Many Two-Disjoint Path Covers in Cylindrical and Toroidal Grids

Jung-Heum Park[a], Insung Ihm[b,*]

[a] *School of Computer Science and Information Engineering*
The Catholic University of Korea, Bucheon, Korea
[b] *Department of Computer Science and Engineering*
Sogang University, Seoul, Korea

Abstract

A many-to-many k-disjoint path cover of a graph joining two disjoint vertex sets S and T of equal size k is a set of k vertex-disjoint paths between S and T that altogether cover every vertex of the graph. The many-to-many k-disjoint path cover is classified as *paired* if each source in S is further required to be paired with a specific sink in T, or *unpaired* otherwise. In this paper, we first establish a necessary and sufficient condition for a bipartite cylindrical grid to have a paired many-to-many 2-disjoint path cover joining S and T. Based on this characterization, we then prove that, provided the set $S \cup T$ contains the equal numbers of vertices from different parts of the bipartition, the bipartite cylindrical grid always has an unpaired many-to-many 2-disjoint path cover. Additionally, we show that such balanced vertex sets also guarantee the existence of a paired many-to-many 2-disjoint path cover for any bipartite toroidal grid even if an arbitrary edge is removed.

Keywords: Disjoint path, path cover, path partition, square grid, lattice graph, cylindrical grid.

1. Introduction

1.1. Many-to-many k-disjoint path covers

In this paper, we consider only a finite simple undirected graph G, whose vertex and edge sets shall be denoted by $V(G)$ and $E(G)$, respectively. For any two vertices u and v in $V(G)$, a path P from u to v in G is a sequence $(w_0, w_1, \ldots, w_n)$ of distinct vertices in $V(G)$ such that $w_0 = u$, $w_n = v$, and w_i and w_{i+1} are adjacent in G for $i \in \{0, \ldots, n-1\}$. If $n \geq 2$ and w_0 and w_n of the sequence are adjacent, the new sequence $(w_0, w_1, \ldots, w_n, w_0)$ is called a cycle. A *path cover* of G is a set of paths in G such that every vertex in $V(G)$ belongs to at least one path. A *vertex-disjoint path cover*, or simply a *disjoint path cover*, of G is a path cover in which every vertex in $V(G)$ is contained in exactly one path.

The major concern of this paper is to study the existence of disjoint path covers for specific classes of graphs, whose paths are additionally required to respectively connect prescribed pairs of distinct vertices. Here, we rephrase the definitions for such constrained disjoint path covers, which were originally given in [37].

*Corresponding author
Email addresses: j.h.park@catholic.ac.kr (Jung-Heum Park), ihm@sogang.ac.kr (Insung Ihm)

Definition 1 (Paired many-to-many k-disjoint path cover). *For a graph G and a positive integer k, let* $S = \{s_1, \ldots, s_k\}$ *and* $T = \{t_1, \ldots, t_k\}$ *be two disjoint subsets of* $V(G)$*. A disjoint path cover* $\{P_1, \ldots, P_k\}$ *of G is called* a paired many-to-many k-disjoint path cover *if* P_i *is a path from* s_i *to* t_i *for every* $i \in \{1, \ldots, k\}$.

Definition 2 (Unpaired many-to-many k-disjoint path cover). *For a graph G and a positive integer k, let* $S = \{s_1, \ldots, s_k\}$ *and* $T = \{t_1, \ldots, t_k\}$ *be two disjoint subsets of* $V(G)$*. A disjoint path cover* $\{P_1, \ldots, P_k\}$ *of G is called* an unpaired many-to-many k-disjoint path cover *if, for some permutation* σ *on* $\{1, \ldots, k\}$, P_i *is a path from* s_i *to* $t_{\sigma(i)}$ *for every* $i \in \{1, \ldots, k\}$.

Here, the vertices in S and T shall be called *sources* and *sinks*, respectively, and *terminals*, collectively, whose meanings are easily understood. The many-to-many k-disjoint path cover of a graph is a path partition whose k paths respectively join the sources to the sinks. As the definitions say, the *paired* many-to-many k-disjoint path cover is more restrictive than the *unpaired* one in the sense that the paired one is an unpaired many-to-many k-disjoint path cover with the condition that only the identity permutation is used. Two simpler variants of these disjoint path covers have been thought in the literature by allowing a single-vertex terminal set: the *one-to-many* k-disjoint path cover for $S = \{s\}$ and $T = \{t_1, \ldots, t_k\}$ and the *one-to-one* k-disjoint path cover for $S = \{s\}$ and $T = \{t\}$, in which their path covers may share the single-vertex terminal(s) only. (Refer to [21, 34, 37, 41] for more details for these variants.)

The concept of the k-disjoint path cover is naturally associated with that of the vertex-connectivity: Menger's theorem explains the connectivity of a graph in terms of the number of internally vertex-disjoint paths (of type one-to-one) joining two distinct vertices, whereas the Fan Lemma describes the connectivity of a graph in terms of the number of internally vertex-disjoint paths (of type one-to-many) joining a vertex to a set of vertices [3]. (Please be aware that, unlike the k-disjoint path cover, the internally vertex-disjoint paths in the theorem and lemma do not have to cover all vertices of the graph.) Moreover, although we do not provide the proof here, it can be shown without a difficulty that a graph is k-connected if and only if it has k vertex-disjoint paths (of type unpaired many-to-many) joining two arbitrary (not necessarily disjoint) vertex sets of size k each, where a vertex that belongs to both sets is considered as a valid, one-vertex path.

The disjoint-path coverability is also closely related to the Hamiltonicity of a graph. For example, a Hamiltonian path between two distinct vertices in a graph forms a many-to-many, one-to-many, and one-to-one 1-disjoint path covers of the graph. A graph is Hamiltonian if and only if it has a one-to-one 2-disjoint path cover for any pair of distinct vertices. Furthermore, a graph of order at least three has a one-to-many 2-disjoint path cover for any terminal sets if and only if it is *Hamiltonian-connected*, that is, every pair of vertices are joined by a Hamiltonian path. Using a disjoint path cover, the construction of a Hamiltonian path or cycle passing through prescribed edges was suggested in [35, 37, 38]. For the problem of Hamiltonian path or cycle through prescribed edges, also refer to [4, 11].

1.2. Rectangular, cylindrical, and toroidal grids

In the context of the Hamiltonian path problem, the rectangular grid graph, or the rectangular grid, first appeared in the literature in [28], which naturally motivated a study on the existence of a 2-disjoint path cover in this graph.

Definition 3 (Rectangular grid). *The* $m \times n$ rectangular grid *G is a graph such that* $V(G) = \{v^i_j : 0 \le i \le m-1, 0 \le j \le n-1\}$ *and* $E(G) = \{(v^i_j, v^{i'}_{j'}) : |i - i'| + |j - j'| = 1\}$.

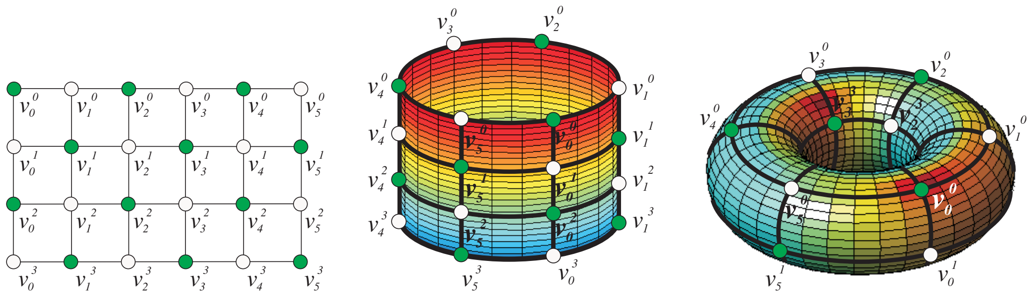

(a) Rectangular (b) Cylindrical (c) Toroidal

Figure 1: Illustrations of rectangular, cylindrical, and toroidal grids of size 4×6.

In the formal definition of the $m \times n$ rectangular grid, the vertices are often chosen from the points of the Euclidean plane with integer coordinates so that the vertices and edges form a rectangular grid with n vertices appearing in each of m rows and m vertices in each of n columns (see Figure 1a). In this paper, however, we simply view it as a graph that is isomorphic to the Cartesian product $P_m \times P_n$ of path graphs on m and n vertices because the actual drawing is irrelevant to our study. The rectangular grid is a bipartite graph and thus its vertices may be colored in two colors, green and white, in such a way that every pair of adjacent vertices is colored differently (hereafter, we will denote the color of vertex v by $c(v) \in \{\mathsf{green}, \mathsf{white}\}$).

Besides the rectangular grid graph, we also consider the following two related classes of grid graphs:

Definition 4 (Cylindrical grid). *The* $m \times n$ cylindrical grid *G is a graph such that* $V(G) = \{v^i_j : 0 \le i \le m-1, 0 \le j \le n-1\}$ *and* $E(G) = \{(v^i_j, v^{i'}_{j'}) : (j = j' \,\&\, |i - i'| = 1)$ *or* $(i = i' \,\&\, j' \equiv j + 1 \pmod{n})\}$.

Definition 5 (Toroidal grid). *The* $m \times n$ toroidal grid *G is a graph such that* $V(G) = \{v^i_j : 0 \le i \le m-1, 0 \le j \le n-1\}$ *and* $E(G) = \{(v^i_j, v^{i'}_{j'}) : (j = j' \,\&\, i' \equiv i+1 \pmod{m})$ *or* $(i = i' \,\&\, j' \equiv j+1 \pmod{n})\}$.

The $m \times n$ cylindrical grid can be constructed from the $m \times n$ rectangular grid by adding horizontal wrap-around edges (v^i_{n-1}, v^i_0) for $i \in \{0, \ldots, m-1\}$ (see Figure 1b). Thus, it is isomorphic to the Cartesian product $P_m \times C_n$ where C_n is a cycle graph on n vertices. The toroidal grid can be generated from the $m \times n$ cylindrical grid by adding vertical wrap-around edges (v^{m-1}_j, v^0_j) for $j \in \{0, \ldots, n-1\}$ (see Figure 1c). Thus, it is isomorphic to the product $C_m \times C_n$ of two cycles. In contrast to the rectangular grid, which is always bipartite, the $m \times n$ cylindrical grid is bipartite if and only if n is even. Furthermore, the $m \times n$ toroidal grid is bipartite if and only if both m and n are even.

1.3. Related works

The disjoint path cover finds applications in many areas such as software testing, database design, and code optimization [2, 32], and is concerned with applications where a full utilization of network nodes in a communication system is important [37]. It has frequently been studied with respect to various graphs such as hypercubes [5, 6, 7, 12, 16, 19, 27], recursive circulants [21, 22, 37, 38], hypercube-like graphs [18, 25, 38], cubes of connected graphs [35, 34], and k-ary n-cubes [41, 44]. Unfortunately, finding a disjoint path cover is not easy. For an arbitrary pair of terminal vertex sets, it is even NP-complete to determine if there exists a many-to-many, one-to-many, or one-to-one k-DPC in a graph for any fixed $k \geq 1$ [37, 38].

On the other hand, due to their regular structures, research works on the properties of the grid graphs are easily found, including the results on Hamiltonian properties [1, 15, 17, 36], disjoint path covers [29, 30], counting structures (e.g., spanning trees, Hamiltonian cycles, etc.) [10, 14], identifying code [20, 26], bandwidth and edge-bandwidth [9, 39], cutwidth and bisection width [40], and pathwidth [13]. Whereas most of the previous investigations dealt with the simple, square grid graph [9, 10, 13, 14, 17, 20, 26, 29, 30, 36, 39, 40], interesting results were also presented for the triangular or hexagonal grid graph, e.g., [1, 15]. In addition, several studies were carried out for the cylindrical grid [10, 13, 14, 36, 40] and the toroidal grid [13, 14, 30, 39, 40].

1.4. Our contributions

The existence of a many-to-many k-disjoint path cover in a graph is fundamentally related to the vertex-connectivity of the graph. Apparently, the rectangular grid does not possess sufficient vertex-connectivity that would always enable to find a desired many-to-many k-disjoint path cover for even a small k. An interesting question is how more easily one can find a many-to-many k-disjoint path cover in the cylindrical or toroidal grid that has slightly higher vertex-connectivity. In this paper, we investigate the structural properties of the still lightly-connected cylindrical or toroidal grid in the point of the existence of a many-to-many k-disjoint path cover. More specifically, we make our endeavor to classify the relative positions of the source and sink vertices that would hinder the existence of a many-to-many 2-disjoint path cover in a *bipartite* cylindrical or toroidal grid, whose two color classes are always the same in size. First, we provide a necessary and sufficient condition for an $m \times n$ cylindrical grid with $m \geq 2$ and even $n \geq 4$ to have a paired many-to-many 2-disjoint path cover joining two terminal sets $S = \{s_1, s_2\}$ and $T = \{t_1, t_2\}$. Second, from this characterization, we derive the fact that an $m \times n$ cylindrical grid has an unpaired many-to-many 2-disjoint path cover joining S and T if and only if the number of terminals that belong to each of the two color classes is the same. Finally, we show that an $m \times n$ toroidal grid with $m, n \geq 4$, both even, has a paired many-to-many 2-disjoint path cover joining S and T despite an arbitrary fault edge if and only if $S \cup T$ contains the same numbers of terminals from different color classes.

2. Preliminaries

2.1. Some useful properties of the grid graphs

Some important Hamiltonian properties of the rectangular and cylindrical grids have been revealed in previous studies, some of which will be effectively used for deriving our results.

Lemma 1 (Chen and Quimpo [8]). *Let G be an $m \times n$ rectangular grid with $m, n \geq 2$. (a) If mn is even, then G has a Hamiltonian path from a corner vertex, i.e., a vertex of degree two, to any other vertex in the different color class. (b) If mn is odd, then G has a Hamiltonian path from a corner vertex to any other vertex in the same color class.*

Consider a connected bipartite graph G with a proper coloring in two colors. The graph G is called *balanced* if its two color classes have equal cardinality. In this paper, we will also call a subset of $V(G)$ *balanced* if the number of vertices in the subset that belong to each of the two color classes is equal. A (balanced) bipartite graph is called *Hamiltonian-laceable* if there is a Hamiltonian path between any two vertices from different color classes [42]. The concept of Hamiltonian-laceability has often been extended in such a way that a bipartite graph whose color classes may differ in cardinality by exactly one is also *Hamiltonian-laceable* if every pair of vertices from the same major color class can be joined by a Hamiltonian path. Finally, a bipartite graph G is called 1*-fault Hamiltonian-laceable* if G remains Hamiltonian-laceable even if a single vertex or edge is deleted from G. Note that, according to these extended definitions, only the class of balanced bipartite graphs may have a chance to be 1-fault Hamiltonian-laceable.

Lemma 2 (Tsai, Tan, Chuang, and Hsu [43]). *An $m \times n$ cylindrical grid with $m \geq 2$ and even $n \geq 4$ is* 1*-fault Hamiltonian-laceable.*

As a further extension of the Hamiltonian-laceability, the strongly Hamiltonian-laceability was derived with respect to the cylindrical grid in [36], according to which the bipartite cylindrical grid is 1-fault strongly Hamiltonian-laceable. On the other hand, for the bipartite toroidal grid, the existence of a paired many-to-many 2-disjoint path cover was investigated by Makino [30], a generalization of whose result will be derived in our work.

Lemma 3 (Makino [30]). *An $m \times n$ toroidal grid with $m, n \geq 4$, both even, has a paired many-to-many* 2*-disjoint path cover for any pair of terminal sets if and only if their union is balanced.*

A necessary and sufficient condition for the existence of a paired many-to-many 2-disjoint path cover in the bipartite toroidal grid, possibly with a single vertex removed, was also studied, where the interested reader is referred to [24]. For the nonbipartite cylindrical or toroidal grid, some properties are already known. Every $m \times n$ cylindrical grid with $m \geq 2$ and odd $n \geq 3$ is Hamiltonian-connected [23, 43]. Also, an $m \times n$ toroidal grid with $m \geq 3$ and odd $n \geq 3$ has a paired many-to-many 2-disjoint path cover joining any pair of source set S and sink set T such that $S \cap T = \emptyset$ [33]. To the best knowledge of the authors of this article, the many-to-many 2-disjoint path cover problem has not previously been studied with respect to the nonbipartite cylindrical grid.

2.2. Further notation and convention

For an $m \times n$ grid graph G, whether rectangular, cylindrical, or toroidal, the ith *row* of G is the vertex set $R_i = \{v^i_j : 0 \leq j \leq n-1\}$, whereas the jth *column* is the vertex set $C_j = \{v^i_j : 0 \leq i \leq m-1\}$, implying v^i_j is the vertex both in the ith row and in the jth column. Thus, an edge joining two vertices in R_i is naturally called a *row edge*, and that joining two vertices in C_j is then called a *column edge*. Based on these notations, we indicate multiple rows and columns respectively as $R_{i,i'} = \bigcup_{i \leq r \leq i'} R_r$ if $i \leq i'$; $R_{i,i'} = \emptyset$ otherwise, and $C_{j,j'} = \bigcup_{j \leq r \leq j'} C_r$ if $j \leq j'$; $C_{j,j'} = \emptyset$ otherwise. We denote by G_i and $G_{i,i'}$ the subgraphs of G induced by R_i and $R_{i,i'}$, respectively. Similarly, G^j and $G^{j,j'}$ respectively indicate the subgraphs induced by C_j and $C_{j,j'}$. Naturally, $G^{j,j'}_{i,i'}$ then denotes the subgraph induced by $R_{i,i'} \cap C_{j,j'}$. All arithmetic on the indices of vertices of the cylindrical and toroidal grids is done modulo n or m as needed. For a path P, $V(P)$ and $E(P)$ will indicate the sets of vertices and edges, respectively, that comprise P. An *s–t path* will also refer to a path that runs from s to t.

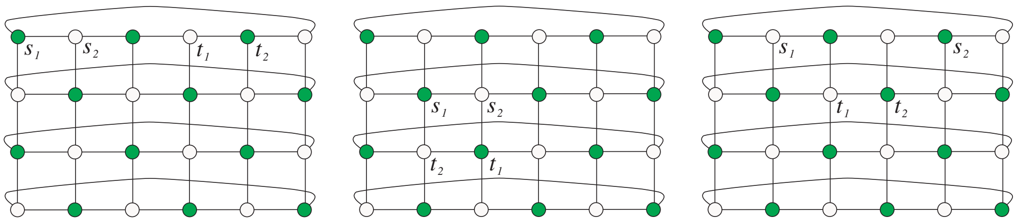

(a) Configuration (A) (b) Configuration (B) (c) Configuration (C)

Figure 2: Three common types of inadmissible configurations.

In this paper, we deal with only the many-to-many type of 2-disjoint path cover, and thus simply call it the 2-disjoint path cover (or the 2-DPC for short) hereafter. In addition, as the definitions of the many-to-many k-disjoint path covers require, it is implicitly assumed that the given source and sink sets, $S = \{s_1, s_2\}$ and $T = \{t_1, t_2\}$, are disjoint.

3. Two-disjoint path covers in cylindrical grids

In this section, we first handle the class of $m \times n$ cylindrical grids with $m \geq 2$ and even $n \geq 4$, which would have a (paired/unpaired) 2-DPC for given terminal sets $S = \{s_1, s_2\}$ and $T = \{t_1, t_2\}$ only if $S \cup T$ is balanced. For effective investigation, we partition the graph class into four subclasses such that (i) $n = 4$, (ii) $m = 2$ & even $n \geq 6$, (iii) $m = 3$ & even $n \geq 6$, and (iv) $m \geq 4$ & even $n \geq 6$. Then, for each subclass of the cylindrical grids, we provide a necessary and sufficient condition for a paired 2-DPC to exist. In addition, we derive an interesting fact that the simple, necessary condition of $S \cup T$ being balanced is sufficient for an unpaired 2-DPC to exist for the entire class of the cylindrical grids.

3.1. Three common types of inadmissible configurations

Before delving into the aforementioned four cases, we first present three fundamental *inadmissible configurations* of the four terminals which would not permit a paired 2-DPC in any $m \times n$ cylindrical grid for $m \geq 2$ and even $n \geq 4$ (refer to Figure 2 for an illustration). These represent rather special cases of inadmissibility conditions from which more general inadmissible configurations are derived for the subclasses of the cylindrical grids in the subsequent subsections.

Theorem 1. *For $m \geq 2$ and even $n \geq 4$, no $m \times n$ cylindrical grid G has a paired 2-DPC joining $S = \{s_1, s_2\}$ and $T = \{t_1, t_2\}$ if S and T form any of the following configurations:*

- **(A)** *$s_1 = v_i^0$, $s_2 = v_p^0$, $t_1 = v_j^0$, and $t_2 = v_q^0$ for some i, j, p, and q such that $i < p < j < q$;*
- **(B)** *$s_1 = v_i^r$, $t_1 = v_{i+1}^{r+1}$, $s_2 = v_{i+1}^r$, and $t_2 = v_i^{r+1}$ for some i and r; and*
- **(C)** *$s_1 = v_i^0$, $t_1 = v_{i+1}^1$, $t_2 = v_{i+2}^1$, and $s_2 = v_{i+3}^0$ for some i.*

Proof. **Proof for (A):** Imagine an annulus, i.e., a region bounded by two concentric circles in a plane, that is topologically equivalent to a cylinder on which G is embedded. Then the curve, homeomorphic to an arbitrary s_1–t_1 path on the cylinder, divides the annulus into two disjoint

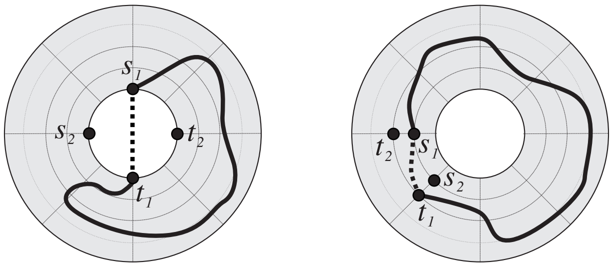

(a) When S and T form a configuration of type (A)

(b) When S and T form a configuration of type (B)

Figure 3: Illustrations for the proof of Theorem 1.

regions (see Figure 3a), which means that the simple closed curve on the plane, obtained by connecting the planar curve via a curve segment outside the annulus, divides the plane into two regions. From the order in which the four terminals are enumerated, we can see that s_2 and t_2 reside in different regions. Then, by the *Jordan curve theorem*, any continuous curve connecting s_2 and t_2 in the annulus must intersect with the closed curve, implying there cannot exist an s_2–t_2 path in G, disjoint from the s_1–t_1 path.

Proof for (B): Similar to the previous proof, imagine a simple closed curve on the plane obtained by connecting the continuous curve, homeomorphic to an arbitrary s_1–t_1 path, via a continuous curve segment inside the region, homeomorphic to the curve quadrilateral on the cylinder, formed by the four terminals (see Figure 3b). Since, again, s_2 and t_2 are separated by the Jordan curve, no 2-DPC may join such S and T.

Proof for (C): In this case, the graph $G \setminus (S \cup T)$ has two connected components, which themselves are balanced bipartite graphs. Since there is no edge in G directly joining any two vertices from different components, the s_1–t_1 path in any 2-DPC must visit all and only all vertices of one connected component. It follows that there must be a Hamiltonian path within that connected component joining two neighbors of s_1 and t_1, which also have the same color. However, this is impossible because any Hamiltonian path in a balanced bipartite graph must join two vertices in different color classes. Thus, there is no desired 2-DPC. □

Note that the inadmissible configurations specified in the theorem have many variants that lead to the same infeasibility. That is, the theorem also holds for the terminal sets, obtained via transforming any of those in the theorem (i) by exchanging $\{s_1, t_1\}$ and $\{s_2, t_2\}$, (ii) by exchanging s_1 and t_1, and/or s_2 and t_2, or (iii) by mapping the original or exchanged set of terminals under an automorphism of the cylindrical grid. For instance, if $t_2 = v_q^{m-1}$, $s_1 = v_i^{m-1}$, $s_2 = v_p^{m-1}$, and $t_1 = v_j^{m-1}$ for some $q < i < p < j$, there also cannot be a paired 2-DPC for the same reason as that specified in (A). From now on, we say that two configurations are *equivalent* to each other if one can be transformed from the other in a way just mentioned above.

Interestingly enough, the three inadmissible configurations, given in Theorem 1, become exactly those for cylindrical grids of large enough dimensions ($m \geq 4$ & even $n \geq 6$), as will be shown in the next theorem.

Theorem 2. *For $m \geq 4$ and even $n \geq 6$, an $m \times n$ cylindrical grid G has a paired 2-DPC joining*

$S = \{s_1, s_2\}$ and $T = \{t_1, t_2\}$ if and only if $S \cup T$ is balanced, and the four terminals in $S \cup T$ do not form an inadmissible configuration equivalent to (A), (B), or (C).

Proof. The necessity part is due to Theorem 1 and the fact that there exists a paired 2-DPC joining S and T in a balanced bipartite graph only if $S \cup T$ is balanced. On the other hand, the sufficiency part proceeds by induction on m. We assume w.l.o.g. that either (i) $|R_{m-1} \cap (S \cup T)| < |R_0 \cap (S \cup T)|$, or (ii) $|R_{m-1} \cap (S \cup T)| = |R_0 \cap (S \cup T)|$ and $|R_{m-2} \cap (S \cup T)| \leq |R_1 \cap (S \cup T)|$. Due to its complexity, the proof for the base step ($m = 4$) is deferred to Theorem 6 in Subsection 3.5, which is in turn based on Theorems 4 and 5 that handle the special classes of cylindrical grids of dimensions $2 \times n$ and $3 \times n$, respectively. From now on, assume that $m \geq 5$ for the inductive step. We construct a proper 2-DPC paths P_1 and P_2, respectively joining s_1 & t_1, and s_2 & t_2, for each of the following three cases.

Case 1: *R_{m-1} has no terminal.* If $G_{0,m-2}$, the subgraph induced by $R_{0,m-2}$, has a paired 2-DPC joining S and T, then it suffices to replace an arbitrary row-$(m-2)$ edge (u, v) comprising a DPC path with the path (u, P_h, v), where P_h is the Hamiltonian path of G_{m-1}, connecting the two neighbors of u and v in R_{m-1}. If there exists no such 2-DPC, S and T must form an inadmissible configuration in $G_{0,m-2}$, which may be equivalent to (A), (B), or (C) by the induction hypothesis. First, the configuration (A) is not possible. Otherwise, the two troublesome cases of $S \cup T \subset R_0$ and $S \cup T \subset R_{m-2}$ would lead us to the contradictions that the terminal sets also form an inadmissible configuration in G, and they violate the assumption (ii), respectively. Second, the same is true for the configuration (B) because, otherwise, the same configuration would also be found in G. Third, the configuration (C) is also impossible. Otherwise, the two troublesome cases of $S \cup T \subset R_0 \cup R_1$ and $S \cup T \subset R_{m-2} \cup R_{m-3}$ also would lead us to the similar contradictions as in the case of (A).

Case 2: *R_{m-1} has a single terminal.* Let the terminal in R_{m-1} be, say, t_2. Then, at least one of the two neighbors in R_{m-2} of the two neighbors in R_{m-1} of t_2 is a nonterminal (otherwise, $S \cup T$ would be unbalanced). Let t_2' be such a nonterminal in R_{m-2}, and x be the common neighbor in R_{m-1} of t_2' and t_2. If $G_{0,m-2}$ has a paired 2-DPC composed of an s_1–t_1 path P_1 and an s_2–t_2' path P_2', then we have a wanted 2-DPC of G, $\{P_1, (P_2', P_h)\}$, where P_h is a Hamiltonian x–t_2 path of G_{m-1}. Such paired 2-DPC of $G_{0,m-2}$ always exists, meaning S and $\{t_1, t_2'\}$ do not form an inadmissible configuration in $G_{0,m-2}$, because R_0 has at least one terminal by the assumption (i) and (ii), and any four terminals forming an inadmissible configuration equivalent to (A), (B), or (C) occupy at most two consecutive rows.

Case 3: *R_{m-1} has two terminals.* First, suppose $s_2 := v_p^{m-1}$ and $t_2 := v_q^{m-1}$ (for some p and q) are the two terminals in R_{m-1}. If we let $s_2' = v_{q-1}^{m-2}$ and $t_2' = v_{p-1}^{m-2}$, there exists a paired 2-DPC in $G_{0,m-2}$ composed of an s_1–t_1 path P_1 and an s_2'–t_2' path P_2' (because $s_1, t_1 \in R_0$ and any inadmissible configuration occupies at most two consecutive rows). Thus, G has a desired 2-DPC $\{P_1, P_2\}$, where P_2 is the concatenation of $(v_p^{m-1}, v_{p+1}^{m-1}, \ldots, v_{q-1}^{m-1})$, P_2', and $(v_{p-1}^{m-1}, v_{p-2}^{m-1}, \ldots, v_q^{m-1})$. (Recall that all arithmetic on the indices of vertices is done modulo n.) Second, suppose $t_1 := v_j^{m-1}$ and $t_2 := v_q^{m-1}$ (for some j and q) are the two terminals in R_{m-1}. If we let $t_1' = v_{q-1}^{m-2}$ and $t_2' = v_{j-1}^{m-2}$, there exists a paired 2-DPC in $G_{0,m-2}$ composed of an s_1–t_1' path P_1' and an s_2–t_2' path P_2'. Then, we have a wanted 2-DPC $\{P_1, P_2\}$, where $P_1 = (P_1', v_{q-1}^{m-1}, v_{q-2}^{m-1}, \ldots, v_j^{m-1})$ and $P_2 = (P_2', v_{j-1}^{m-1}, v_{j-2}^{m-1}, \ldots, v_q^{m-1})$. This completes the proof. □

Corollary 1. *For $m \geq 4$ and even $n \geq 6$, an $m \times n$ cylindrical grid G has an unpaired 2-DPC joining $S = \{s_1, s_2\}$ and $T = \{t_1, t_2\}$ if and only if $S \cup T$ is balanced.*

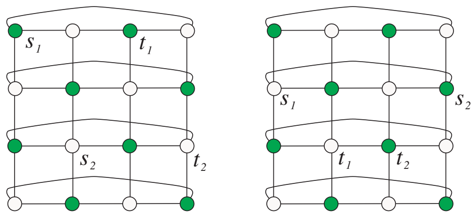

(a) Configuration (A1) (b) Configuration (C1)

Figure 4: Examples of inadmissible configurations for $m \times 4$ cylindrical grids with $m \geq 2$.

Proof. The necessity part is straightforward. For the sufficiency part, if G has a paired 2-DPC joining S and T, it is also a desired unpaired 2-DPC. If G does not have a paired 2-DPC even though $S \cup T$ is balanced, S and T form an inadmissible configuration equivalent to (A), (B), or (C) by Theorem 2. Then, for the new sink set $T' := \{t'_1, t'_2\}$ with $t'_1 = t_2$ and $t'_2 = t_1$, it is straightforward to see that S and T' satisfy the condition of Theorem 2, implying the existence of a paired 2-DPC composed of s_1–t'_1 and s_2–t'_2 paths. Therefore, we have an unpaired 2-DPC joining S and T, completing the proof. □

3.2. 2-DPCs in $m \times 4$ cylindrical grids with $m \geq 2$

Consider the cylindrical grids with at least two rows and exactly four columns. For this type of cylindrical grids, two new inadmissible configurations, (A1) and (C1), are introduced, which will be defined in the next lemma (see Figure 4). Recall that the aforementioned configurations (A) and (C) are just special cases of (A1) and (C1), respectively.

Lemma 4. *For $m \geq 2$, no $m \times 4$ cylindrical grid G has a paired 2-DPC joining $S = \{s_1, s_2\}$ and $T = \{t_1, t_2\}$ if S and T form any of the following configurations:*

- **(A1)** $s_1, t_1 \in R_{r_1}$, $s_2, t_2 \in R_{r_2}$, *and* $c(s_1) = c(t_1) \neq c(s_2) = c(t_2)$ *for some* r_1 *and* r_2*; and*
- **(C1)** $s_1 = v^r_i$, $t_1 = v^{r+1}_{i+1}$, $t_2 = v^{r+1}_{i+2}$, *and* $s_2 = v^r_{i+3}$ *for some* i *and* r.

Proof. **Proof for (A1):** Suppose for a contradiction that there exists a paired 2-DPC composed of an s_1–t_1 path P_1 and an s_2–t_2 path P_2. We first claim that $|V(P_1) \cap R_j| \neq 1$ for every row j. Suppose otherwise, i.e., $V(P_1) \cap R_j = \{x\}$ for some index $j\,(\neq r_1)$ and vertex x. Starting from s_1, if P_1 visits x from below (resp. above), it must also visit a vertex $y \in R_j$ other than x on the way down (resp. up) to t_2, leading to a contradiction, and proving the claim. A similar argument leads to the fact that $|V(P_2) \cap R_j| \neq 1$ for every row j. It follows that $|V(P_1) \cap R_j|$ is even for every row j (because $|V(P_1) \cap R_j| \neq 1, 3$), and thus $|V(P_1)|$ is even. This is impossible because P_1 is a path joining two terminals of the same color.

Proof for (C1): Again, G becomes separated by the four terminals into two balanced bipartite connected components. Thus, similar to the proof for the configuration (C) of Theorem 1, we can show that no desired 2-DPC can exist since $c(s_1) = c(t_1) \neq c(s_2) = c(t_2)$. □

Now, we are ready to specify the exact condition that allows a paired 2-DPC joining given source and sink sets in the current class of cylindrical graphs.

Theorem 3. *For $m \geq 2$, an $m \times 4$ cylindrical grid G has a paired 2-DPC joining $S = \{s_1, s_2\}$ and $T = \{t_1, t_2\}$ if and only if $S \cup T$ is balanced, and the four terminals in S and T do not form an inadmissible configuration equivalent to (A1), (B), or (C1).*

Proof. The necessity part is due to Theorem 1 and Lemma 4 (and the fact that there exists a paired 2-DPC joining S and T in a balanced bipartite graph only if $S \cup T$ is balanced). The sufficiency proof is by induction on m, in which the proof for the base case of $m = 2$ is deferred to the Appendix section. For the inductive step of $m \geq 3$, assume w.l.o.g. that $|R_{m-1} \cap (S \cup T)| \leq |R_0 \cap (S \cup T)|$, i.e., there are no more terminals in R_{m-1}, if any, than in R_0. We have three cases.

Case 1: *R_{m-1} has no terminal.* By the induction hypothesis, $G_{0,m-2}$, the $(m-1) \times 4$ cylindrical grid induced by $R_{0,m-2}$, has a paired 2-DPC $\{P'_1, P'_2\}$ joining S and T. If, for some $i \in \{1, 2\}$, P'_i that joins s_i and t_i passes through an edge (u, v) of G_{m-2}, then P'_i can be represented as $(s_i, P_u, u, v, P_v, t_i)$ for some subpaths P_u and P_v in $G_{0,m-2}$. Since G_{m-1}, a length-four cycle, is Hamiltonian-laceable, P_i and P'_{3-i} form a desired 2-DPC of G, where $P_i = (s_i, P_u, u, P_h, v, P_v, t_i)$ for the Hamiltonian path P_h of G_{m-1} joining the neighbors of u and v in R_{m-1}.

If no path in the 2-DPC of $G_{0,m-2}$ passes through an edge of G_{m-2}, the only possibility is that $S \cup T = R_{m-2}$. Furthermore, since no configuration equivalent to (A1) is possible, it should be that s_1 and t_1, and s_2 and t_2 are adjacent to each other in G_{m-2}. Note that $G_{0,m-3}$ and G_{m-1} are either a four-column cylindrical grid with multiple rows or a length-four cycle, and thus Hamiltonian-laceable (the former is due to Lemma 2). Hence, we can find a desired 2-DPC of G, $\{P_1, P_2\}$, where P_1 is built by connecting s_1 and t_1 through a Hamiltonian path of $G_{0,m-3}$ joining the two neighbors of s_1 and t_1, both in R_{m-3}, and P_2, similarly via a Hamiltonian path of G_{m-1}.

Case 2: *R_{m-1} has one terminal.* Assume w.l.o.g. that $t_2 \,(:= v^{m-1}_q) \in R_{m-1}$, and further let $x = v^{m-2}_{q-1}$ and $y = v^{m-2}_{q+1}$, in which $c(x) = c(y) = c(t_2)$. If $s_2 \in \{x, y\}$, say $x = s_2$, then we can find a paired 2-DPC $\{P_1, P_2\}$ of G in such a way that P_1 is a Hamiltonian s_1–t_1 path of $G_{0,m-2} \setminus x$, which exists due to Lemma 2, and P_2 is s_2, followed by the Hamiltonian v^{m-1}_{q-1}–t_2 path of G_{m-1}. Suppose then $s_2 \notin \{x, y\}$. Clearly, at least one of x and y is a nonterminal, or $S \cup T$ would not be balanced. Then we claim that we can always choose a nonterminal t'_2 from $\{x, y\}$ such that S and $T' := \{t_1, t'_2\}$ do not violate the conditions of the theorem with respect to $G_{0,m-2}$: if one of x and y is either s_1 or t_1, it suffices to let the other nonterminal be t'_2. If both of x and y are nonterminals, we can also choose such t'_2 from $\{x, y\}$ so that the conditions are not violated whether there is a single terminal (other than x and y) in R_{m-2} or not. Therefore, by the induction hypothesis, there exists a paired 2-DPC in $G_{0,m-2}$, made of an s_1–t_1 path, P_1, and an s_2–t'_2 path, P'_2. Then, P_1 and P_2, which is P'_2, followed by the Hamiltonian path of G_{m-1} joining the neighbor of t'_2 in R_{m-1} and t_2, form a desired 2-DPC of G.

Case 3: *R_{m-1} has two terminals.* In this case, by the assumption of the proof, there exist two terminals also in R_0. For the first subcase, assume w.l.o.g. that $s_2, t_2 \in R_{m-1}$. Then, $c(s_2) \neq c(t_2)$ (and hence $c(s_1) \neq c(t_1)$ in R_0), or S and T would satisfy a condition equivalent to (A1). Hence, the 2-DPC of G can be built by finding a Hamiltonian s_1–t_1 path in $G_{0,m-2}$ and a Hamiltonian s_2–t_2 path in G_{m-1}, which exist clearly. For the second subcase, assume w.l.o.g. that $t_1, t_2 \in R_{m-1}$. We claim there exists an ordered pair (x, y) of vertices in R_{m-2} such that (i) $G_{0,m-2}$ has a paired 2-DPC composed of s_1–x path and s_2–y path and (ii) G_{m-1} has two disjoint paths, x'–t_1 path and y'–t_2 path, covering every vertex of G_{m-1}, where x' is the neighbor of x in R_{m-1} and y' is the neighbor of y in R_{m-1}, and x'–t_1 path or y'–t_2 path might be a one-vertex path. Note that, since G_{m-1} is isomorphic to a cycle of length four, there exist three (resp. two) ordered pairs (x', y') in R_{m-1} that satisfy (ii) if $(t_1, t_2) \in E(G)$ (resp. $(t_1, t_2) \notin E(G)$). Thus, it is always

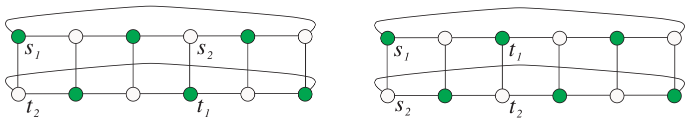

(a) Configuration (B2)

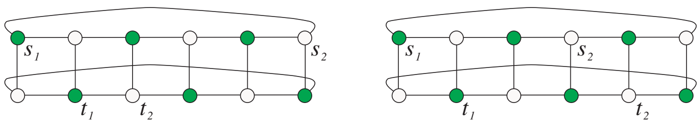

(b) Configuration (C2)

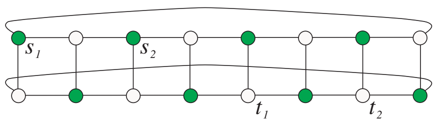

(c) Configuration (D2)

Figure 5: Examples of inadmissible configurations for $2 \times n$ cylindrical grids with $n \geq 6$.

possible to choose (x, y) such that any inadmissible configuration equivalent to (B) or (C1) can be avoided even when $m = 3$ (recall the assumption made in this second subcase, which would also not permit an inadmissible configuration equivalent to (A1)). Once the claim is true, we can build a desired 2-DPC of G by concatenating the s_1–x and x'–t_1 paths and the s_2–y and y'–t_2 paths, respectively. The proof is completed. □

Corollary 2. *For $m \geq 2$, an $m \times 4$ cylindrical grid G has an unpaired 2-DPC joining $S = \{s_1, s_2\}$ and $T = \{t_1, t_2\}$ if and only if $S \cup T$ is balanced.*

Proof. If $S \cup T$ is balanced, and there is no paired 2-DPC of G joining S and T, then S and T form an inadmissible configuration equivalent to (A1), (B), or (C1) by Theorem 3. In this case, we can find a paired 2-DPC composed of an s_1–t_2 path and an s_2–t_1 path by breaking the inadmissibility condition through an exchange of t_1 and t_2. Thus, there exists a wanted unpaired 2-DPC. The corollary follows. □

3.3. 2-DPCs in $2 \times n$ cylindrical grids with even $n \geq 6$

For the specific group of cylindrical grids having exactly two rows, we find that three more general classes of inadmissible configurations exist as presented in the following lemma (see Figure 5). Note that the aforementioned inadmissible configurations (B) and (C) are just special cases of (B2) and (C2), respectively.

Lemma 5. *For even $n \geq 6$, no $2 \times n$ cylindrical grid G has a paired 2-DPC joining $S = \{s_1, s_2\}$ and $T = \{t_1, t_2\}$ if S and T form any of the following configurations:*

- **(B2)** $S \cup T = \{v_i^0, v_i^1, v_j^0, v_j^1\}$ *and* $c(s_1) = c(t_1) \neq c(s_2) = c(t_2)$ *for some i and j with $i \neq j$;*
- **(C2)** $s_1 = v_i^0$, $t_1 = v_j^1$, $s_2 = v_p^0$, $t_2 = v_q^1$, *and* $c(s_1) = c(t_1) \neq c(s_2) = c(t_2)$ *for some i, j, p, and q such that* $\max\{i, j\} < \min\{p, q\}$*; and*

(D2) *$s_1 = v_i^0$, $s_2 = v_p^0$, $t_1 = v_j^1$, $t_2 = v_q^1$, and $c(s_1) = c(s_2) \neq c(t_1) = c(t_2)$ for some i, j, p, and q such that $i < p < j < q$.*

Proof. **Proof for (B2):** If the ith and jth columns are adjacent to each other, the configuration (B2) is identical to (B), implying that no such 2-DPC exists by Theorem 1. If not, the four terminals separate G into two balanced bipartite graphs. Since $c(s_1) = c(t_1) \neq c(s_2) = c(t_2)$ again, no wanted 2-DPC may exist (refer to the proof for the configuration (C) of Theorem 1).

Proof for (C2): Suppose to the contrary that there exists a wanted paired 2-DPC, composed of an s_1–t_1 path P_1 and an s_2–t_2 path P_2. We first claim that P_1 passes through both $\alpha := v_i^1$ and $\beta := v_j^0$, where it is clear that $(\alpha, \beta) \notin E(G)$ and $c(\alpha) = c(\beta)$. Consider the two columns numbered $i' := \min\{i, j\}$ and $j' := \max\{i, j\}$. If they are adjacent to each other, i.e., $j' = i' + 1$, α and β respectively have only one neighbor other than s_1 and t_1, implying they can only be visited by P_1. If not, i.e., $j' > i' + 1$, they separate G into two balanced, connected components, H, induced by $C_{i'+1,j'-1}$, and H', induced by $C_{0,i'-1} \cup C_{j'+1,n-1}$. Since both s_2 and t_2 are in H', and P_2 may visit H only through α or β, it must visit either both of them or neither of them. Suppose the first. Note that P_2 cannot cover all vertices in H because $c(\alpha) = c(\beta)$. Since P_1 must visit some of them, and thus may not visit H', P_1 and the α–β subpath of P_2 must form a paired 2-DPC of the subgraph, H_1, induced by $C_{i',j'}$, which is impossible because two pairs of corner vertices of a rectangular grid, each of which are diagonally opposite, may not be joined by two disjoint paths. Hence, the claim is proved. Similarly, we can also prove a symmetric claim that P_2 passes through v_p^1 and v_q^0. Now, these two claims imply that P_1 must cover all vertices of H_1 and cannot visit a vertex in $C_{p',q'}$ for $p' := \min\{p, q\}$ and $q' := \max\{p, q\}$. Hence, if P_1 ever visits a vertex outside H_1 after s_1, it must come back to H_1 through α after visiting an even number of vertices since $c(s_1) \neq c(\alpha)$. The same argument is true between t_1 and β, indicating that P_1 is made of an even number of vertices. However, this is impossible because $c(s_1) = c(t_1)$, leading to a contradiction.

Proof for (D2): Again, suppose to the contrary that there exists a wanted paired 2-DPC, $\{P_1, P_2\}$. Let $\alpha = v_p^1$ and $\beta = v_q^0$, in which $(\alpha, \beta) \notin E(G)$ and $c(\alpha) \neq c(\beta)$. Then, $G \setminus \{s_2, t_2, \alpha, \beta\}$ has two balanced, connected components, H, induced by $C_{0,p-1} \cup C_{q+1,n-1}$, and H', induced by $C_{p+1,q-1}$. Since s_1 and t_1 now reside in different components, P_1, the s_1–t_1 path, must visit either α or β, but not both. Suppose first that P_1 passes through α. With $\alpha' := v_{p-1}^1$ and $\alpha'' := v_{p+1}^1$, P_1 can be broken into an s_1–α' path in H, the single-vertex path α, and an α''–t_1 path in H'. Since $c(\alpha') = c(s_1)$ and H is balanced, P_2, the s_2–t_2 path, must also visit H. The subpath(s) of P_2 contained in H should be unique and moreover, run between two vertices whose colors are different from $c(s_1)$. Thus, there remains only one possibility: consider the subpath of P_2 joining s_2' and β' in H, where s_2' and β' are the respective neighbors of s_2 and β in H. Then, the s_1–α' subpath of P_1 and the s_2'–β' subpath of P_2 form a paired 2-DPC of H. However, this is impossible because the s_1–α' path separates H, a rectangular grid, into two connected components, and s_2' and β' reside in different components, leading to a contradiction. In the other case that P_1 passes through β, a similar argument with a β''–t_1 subpath of P_1 and an α''–t_2'' subpath of P_2 that form a paired 2-DPC of H', where β'', α'', and t_2'' are the respective neighbors of β, α, and t_2 in H', also leads us to a contradiction, completing the proof. □

Now, we are ready to present the exact condition for the existence of a paired 2-DPC joining given sets of sources and sinks.

Theorem 4. *For even $n \geq 6$, a $2 \times n$ cylindrical grid G has a paired 2-DPC joining $S = \{s_1, s_2\}$ and $T = \{t_1, t_2\}$ if and only if $S \cup T$ is balanced, and the four terminals in S and T do not form an inadmissible configuration equivalent to (A), (B2), (C2), or (D2).*

Proof. The necessity part is by Theorem 1 and Lemma 5. The sufficiency part proceeds by induction on n, in which the base case of $n = 6$ is deferred to the Appendix section. For the inductive step of $n \geq 8$, the proof considers two cases.

First, assume that there is a pair of consecutive columns of G that contain no terminal. Let r be a column number such that $C_{r,r+1} \cap (S \cup T) = \emptyset$. Then, we can further assume $C_{r-1} \cup C_{r+2} \neq S \cup T$. Otherwise, there would be at least four consecutive empty columns, and we could choose the column numbered, say, $r + 3$ instead. Let H be the $2 \times (n-2)$ cylindrical grid, obtained from G by the deleting vertices of $C_{r,r+1}$ and then adding two *virtual* edges (v^0_{r-1}, v^0_{r+2}) and (v^1_{r-1}, v^1_{r+2}). Since the sufficient condition of the theorem still holds for H, it has a paired 2-DPC, joining S and T by the induction hypothesis. If both virtual edges are passed through by some path(s) in the 2-DPC of H, a 2-DPC of G can be easily constructed by replacing the respective edge with subpaths $(v^0_{r-1}, v^0_r, v^0_{r+1}, v^0_{r+2})$ and $(v^1_{r-1}, v^1_r, v^1_{r+1}, v^1_{r+2})$. If exactly one of them, say (v^0_{r-1}, v^0_{r+2}), is passed through by some path in the 2-DPC of H, it suffices to replace the edge with $(v^0_{r-1}, v^0_r, v^1_r, v^1_{r+1}, v^0_{r+1}, v^0_{r+2})$. Finally, suppose that neither of them are covered by the 2-DPC of H. In this case, we can choose a nonterminal vertex from $C_{r-1} \cup C_{r+2}$, say v^0_{r-1} w.l.o.g., where (v^0_{r-1}, v^1_{r-1}) must be covered by the 2-DPC of H. It suffices to replace the edge with $(v^0_{r-1}, v^0_r, v^0_{r+1}, v^1_{r+1}, v^1_r, v^1_{r-1})$.

Suppose next that every pair of consecutive columns contain a terminal, which falls into the case of $n = 8$. If we assume w.l.o.g. that C_0, C_2, C_4, and C_6 respectively contains one terminal, and $s_1 = v^0_0 \in C_0$, then there are four cases up to symmetry: $t_1 = v^0_2$, v^1_2, v^0_4, or v^1_4: First, if $t_1 = v^0_2$, and thus $\{s_2, t_2\} = \{v^1_4, v^1_6\}$ because $S \cup T$ is balanced, then P_1 is (v^0_0, v^0_1, v^0_2) and P_2 is $(P_x, v^1_2, v^1_1, v^1_0, P_y)$, where P_x is a Hamiltonian v^1_4–v^1_3 path of $G^{3,4}$ and P_y is a Hamiltonian v^1_7–v^1_6 path of $G^{5,7}$ (recall that G^{r_1,r_2} denotes the subgraph induced by C_{r_1,r_2}). Second, if $t_1 = v^1_2$, and thus $\{s_2, t_2\} = \{v^0_4, v^1_6\}$ or $\{v^1_4, v^0_6\}$, then P_1 is a Hamiltonian s_1–t_1 path in $G^{0,3}$ and P_2 is a Hamiltonian s_2–t_2 path in $G^{4,7}$. Third, if $t_1 = v^0_4$, and thus $\{s_2, t_2\} = \{v^1_2, v^1_6\}$, then P_1 is $(P_x, v^0_2, v^0_3, v^0_4)$, where P_x is a Hamiltonian v^0_0–v^0_1 path in $G^{0,1}$, and P_2 is $(v^1_2, v^1_3, v^1_4, P_y)$, where P_y is a Hamiltonian v^1_5–v^1_6 path in $G^{5,7}$. Finally, if $t_1 = v^1_4$, and thus $\{s_2, t_2\} = \{v^0_2, v^1_6\}$ or $\{v^1_2, v^0_6\}$, then S and T form an inadmissible configuration equivalent to (D2) (for $\{s_2, t_2\} = \{v^1_2, v^0_6\}$, consider an automorphism ϕ such that $\phi(v^i_0) = v^i_0$ and $\phi(v^i_j) = v^i_{n-j}$ for $i \in \{0, 1\}$ and $j \in \{1, \ldots, n-1\}$). Therefore, we complete the proof. □

Now, the proof of the next corollary is the same as that of Corollary 2 except that the inadmissible configurations (A), (B2), (C2), and (D2) of Theorem 4 are involved instead.

Corollary 3. *For even $n \geq 6$, a $2 \times n$ cylindrical grid G has an unpaired 2-DPC joining $S = \{s_1, s_2\}$ and $T = \{t_1, t_2\}$ if and only if $S \cup T$ is balanced.*

3.4. 2-DPCs in $3 \times n$ cylindrical grids with even $n \geq 6$

In the case of the $3 \times n$ cylindrical grids with even $n \geq 6$, the set of involved inadmissible configurations become more complicated, in which four new ones (C3), (D3), (E3), and (F3) that will be defined in Lemmas 6 and 7 are considered (refer to Figures 6 and 14 for intuitive illustrations).

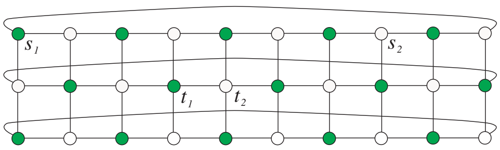

(a) Configuration (C3)

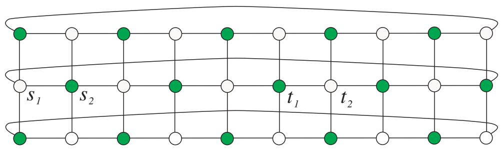

(b) Configuration (D3)

Figure 6: Examples of two inadmissible configurations for $3 \times n$ cylindrical grids with even $n \geq 6$. For (C3) and (D3), the path segments of the s_1–t_1 and s_2–t_2 paths that visit the six vertices in the two consecutive columns containing t_1 and t_2 play a key role in deriving our results.

Lemma 6. *For even $n \geq 6$, no $3 \times n$ cylindrical grid G has a paired 2-DPC joining $S = \{s_1, s_2\}$ and $T = \{t_1, t_2\}$ if S and T form any of the following configurations:*

- **(C3)** *$s_1 = v_i^0$, $t_1 = v_j^1$, $t_2 = v_q^1$, $s_2 = v_p^0$, and $c(s_1) = c(t_1) \neq c(s_2) = c(t_2)$ for some i, j, p, and q such that $i < j < q < p$, $q = j + 1$, and $(n - 1 - p) + i \geq 2$; and*
- **(D3)** *$s_1 = v_i^1$, $s_2 = v_p^1$, $t_1 = v_j^1$, $t_2 = v_q^1$, and $c(s_1) = c(t_2) \neq c(t_1) = c(s_2)$ for some i, j, p, and q such that $i < p < j < q$, $p = i + 1$, and $q = j + 1$.*

Proof. Suppose for a contradiction that there exists a paired 2-DPC composed of an s_1–t_1 path P_1 and an s_2–t_2 path P_2. First, consider the path segments of P_1 and P_2 that pass through the six vertices of $C_{j,j+1}$, where $t_1 = v_j^1$, $t_2 = v_{j+1}^1$, and $s_1, s_2 \notin C_{j,j+1}$, for the configurations (C3) and (D3). We use a 2×2 $(1, 2)$-matrix $M = \left(\begin{smallmatrix} a_{11} & a_{12} \\ a_{21} & a_{22} \end{smallmatrix}\right)$ that indicates the path to which each of the four nonterminals of $C_{j,j+1}$ belongs, where $a_{11} = 1$ iff $v_j^0 \in V(P_1)$; $a_{12} = 1$ iff $v_{j+1}^0 \in V(P_1)$; $a_{21} = 1$ iff $v_j^2 \in V(P_1)$; and $a_{22} = 1$ iff $v_{j+1}^2 \in V(P_1)$.

We make **Claim 1** that, among a total of 2^4 candidates for M, the following five may not happen: $\left(\begin{smallmatrix} 2 & 1 \\ * & * \end{smallmatrix}\right)$, $\left(\begin{smallmatrix} * & * \\ 2 & 1 \end{smallmatrix}\right)$, $\left(\begin{smallmatrix} 1 & 2 \\ 1 & 2 \end{smallmatrix}\right)$, $\left(\begin{smallmatrix} 2 & * \\ 2 & * \end{smallmatrix}\right)$, and $\left(\begin{smallmatrix} * & 1 \\ * & 1 \end{smallmatrix}\right)$, where the elements denoted by $*$ can have arbitrary values in $\{1, 2\}$. To prove this claim, suppose $M = \left(\begin{smallmatrix} 2 & 1 \\ * & * \end{smallmatrix}\right)$ first (see Figure 7a). Then, v_j^0 cannot be an intermediate vertex of P_2 since its two neighbors t_1 and v_{j+1}^0 are vertices of P_1, leading to a contradiction. Similarly, supposing $M = \left(\begin{smallmatrix} * & * \\ 2 & 1 \end{smallmatrix}\right)$ leads to a contradiction. Suppose $M = \left(\begin{smallmatrix} 1 & 2 \\ 1 & 2 \end{smallmatrix}\right)$ (see Figure 7b). Then, (v_j^0, v_j^1) must be an edge of P_1 since v_j^0 is an intermediate vertex of P_1. Also, (v_j^1, v_j^2) must be an edge of P_1. This is impossible, however, since t_1 is a terminal of P_1. Now, suppose $M = \left(\begin{smallmatrix} 2 & * \\ 2 & * \end{smallmatrix}\right)$ (see Figure 7c). Then, (v_j^1, v_{j-1}^1) is an edge of P_1 whereas (v_j^0, v_{j-1}^0) and (v_j^2, v_{j-1}^2) are edges of P_2. This forces (v_{j-1}^1, v_{j-2}^1) to be an edge of P_1 and (v_{j-1}^0, v_{j-2}^0) and (v_{j-1}^2, v_{j-2}^2) to be edges of P_2. Eventually, (v_{i+1}^0, v_i^0) must be an edge of P_2 for the configuration (C3), which is impossible since $v_i^0 = s_1$, or (v_{p+1}^1, v_p^1) must be an edge of P_1 for the configuration (D3), which is also impossible since $v_p^1 = s_2$. Similarly, supposing $M = \left(\begin{smallmatrix} * & 1 \\ * & 1 \end{smallmatrix}\right)$ leads to a contradiction that (v_{p-1}^0, v_p^0) is an edge of P_1 for the configuration (C3) whereas (v_{i-1}^1, v_i^1) is an edge of P_2 for the configuration (D3). Thus, the claim is proved.

As a result, we now have the only six candidates for M: $X1 := \left(\begin{smallmatrix} 1 & 1 \\ 1 & 2 \end{smallmatrix}\right)$, $X2 := \left(\begin{smallmatrix} 1 & 2 \\ 1 & 1 \end{smallmatrix}\right)$, $Y1 := \left(\begin{smallmatrix} 1 & 1 \\ 2 & 2 \end{smallmatrix}\right)$, $Y2 := \left(\begin{smallmatrix} 2 & 2 \\ 1 & 1 \end{smallmatrix}\right)$, $Z1 := \left(\begin{smallmatrix} 1 & 2 \\ 2 & 2 \end{smallmatrix}\right)$, and $Z2 := \left(\begin{smallmatrix} 2 & 2 \\ 1 & 2 \end{smallmatrix}\right)$, for each of them we can construct the path segments of P_1 and P_2 that pass through the vertices of $C_{j,j+1}$, as shown in Figure 8. For the type $X1$, (v_j^1, v_j^2) and (v_j^2, v_{j-1}^2) should be edges of P_1 since v_j^2 is an intermediate vertex of P_1. Similarly, (v_{j+1}^1, v_{j+1}^2) and (v_{j+1}^2, v_{j+2}^2) are edges of P_2. In addition, $(v_{j-1}^0, v_j^0, v_{j+1}^0, v_{j+2}^0)$ should

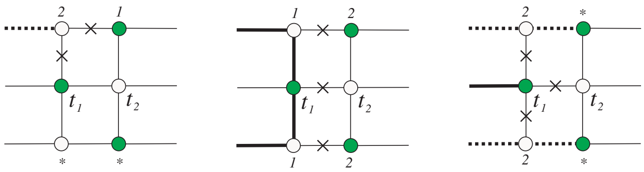

(a) (b) (c)

Figure 7: Illustrations for the proof of Claim 1 in the proof of Lemma 6.

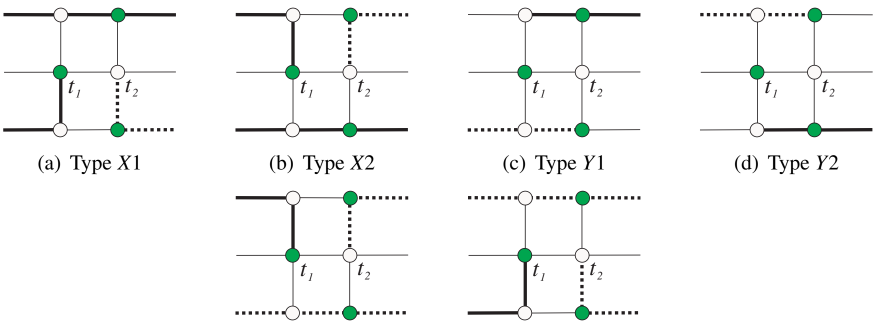

(a) Type $X1$ (b) Type $X2$ (c) Type $Y1$ (d) Type $Y2$

(e) Type $Z1$ (f) Type $Z2$

Figure 8: Six types of path segments in P_1 and P_2, passing through the vertices of $C_{j,j+1}$. Here, edges of P_1 are shown in thick solid lines, whereas those of P_2 are shown in thick dotted lines.

be path segments of P_1 since $(v_j^0, v_j^1), (v_{j+1}^0, v_{j+1}^1) \notin E(P_1) \cup E(P_2)$. In a similar way, the path segments shown in the figure can be obtained for the types other than $X1$. It is worth noting that for the type $Y1$, (t_1, v_j^0) is an edge of P_1 or both (t_1, v_{j-1}^1) and (v_j^0, v_{j-1}^0) are edges of P_1; (t_2, v_{j+1}^2) is an edge of P_2 or both (t_2, v_{j+2}^1) and (v_{j+1}^2, v_{j+2}^2) are edges of P_2. A similar argument applies to the type $Y2$.

Now, let S and T form the configuration (C3). We first investigate whether there can ever exist disjoint s_1–t_1 and s_2–t_2 paths for each of the six types of M, apart from the covering property of the 2-DPC. Assume the $3 \times n$ cylindrical grid is embedded on an annulus, where the row 0 is mapped to the innermost circle, as shown in Figure 9. We easily find that, except for the two types, $X2$ and $Z1$, there may not exist disjoint s_1–t_1 and s_2–t_2 paths. (This fact can be shown by using the Jordan curve theorem, similar to the proof of Theorem 1.) Furthermore, the embedding of two paths for each of the types $X2$ and $Z1$ is unique up to topological equivalence.

For type $X2$, there can exist two disjoint s_1–t_1 path P_1 and s_2–t_2 path P_2 as shown in Figure 9b. Here, we make **Claim 2** that $(v_{p-1}^0, v_p^0) \in E(P_2)$ and $(v_{p-1}^2, v_p^2) \in E(P_1)$ for the two paths to cover every vertex of the graph. If $p = q+1$, we have nothing to prove. Let $p > q+1$. The vertex v_{q+1}^1 to the right of t_2 is an intermediate vertex either of P_1 or of P_2. If the vertex is contained in P_1, as shown in Figure 10a, then $(v_{q+1}^2, v_{q+1}^1), (v_{q+1}^1, v_{q+2}^1) \in E(P_1)$ and $(v_{q+1}^0, v_{q+2}^0) \in E(P_2)$ and thus $(v_{q+2}^1, v_{q+2}^2), (v_{q+2}^2, v_{q+3}^2) \in E(P_1)$ and $(v_{q+2}^0, v_{q+3}^0) \in E(P_2)$. Similarly, if the vertex v_{q+1}^1 is contained in P_2, as shown in Figure 10b, then $(v_{q+2}^2, v_{q+3}^2) \in E(P_1)$ and $(v_{q+2}^0, v_{q+3}^0) \in E(P_2)$. We

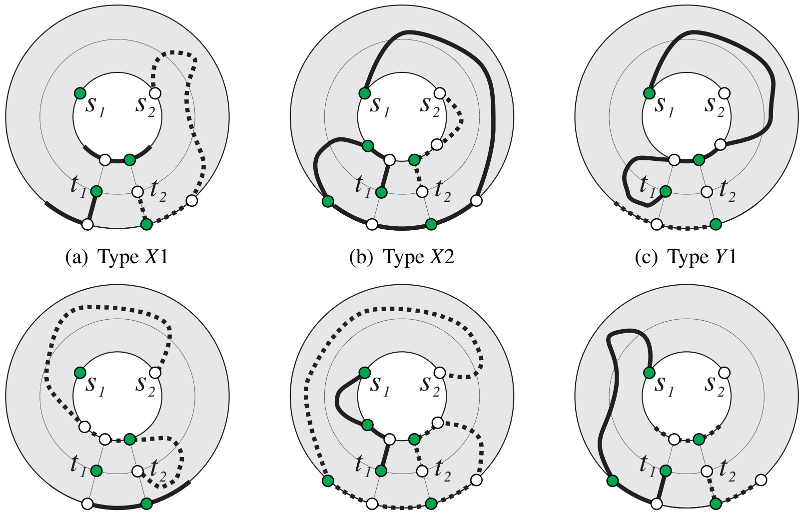

(a) Type $X1$ (b) Type $X2$ (c) Type $Y1$

(d) Type $Y2$ (e) Type $Z1$ (f) Type $Z2$

Figure 9: Embeddings of the s_1–t_1 and s_2–t_2 paths into an annulus for the configuration (C3).

say that (v^2_q, v^2_{q+1}) of P_1 and (v^0_q, v^0_{q+1}) of P_2 forces $(v^2_{q+2}, v^2_{q+3}) \in E(P_1)$ and $(v^0_{q+2}, v^0_{q+3}) \in E(P_2)$. In the same way, we can see that (v^2_{q+2}, v^2_{q+3}) and (v^0_{q+2}, v^0_{q+3}) forces $(v^2_{q+4}, v^2_{q+5}) \in E(P_1)$ and $(v^0_{q+4}, v^0_{q+4}) \in E(P_2)$ and eventually forces $(v^0_{p-1}, v^0_p) \in E(P_2)$ and $(v^2_{p-1}, v^2_p) \in E(P_1)$. Thus the claim is proved.

Now, the vertex v^1_p below s_2 is an intermediate vertex of P_1. It follows that (v^2_p, v^1_p) and (v^1_p, v^1_{p+1}) are edges of P_1. Moreover, for P_1 to cover v^0_{p+1}, (v^1_{p+1}, v^0_{p+1}) should be an edge of P_1; for P_1 to cover v^2_{p+1}, (v^1_{p+1}, v^2_{p+1}) should also be an edge of P_1. Note that v^0_{p+1} and v^2_{p+1} are both nonterminals due to the condition of $(n-1-p)+i \geq 2$. However, the two cases cannot occur simultaneously. Therefore, there can exist no paired 2-DPC for the type $X2$. A symmetric argument applies for the type $Z1$, as illustrated in Figure 10c.

Finally, suppose that S and T form the configuration (D3), where $s_1 = v^1_i$, $s_2 = v^1_{i+1}$, and $t_1, t_2 \notin C_{i,i+1}$. Due to Claim 1, there are also six types of path segments of P_1 and P_2 that passes through $C_{i,i+1}$, as shown in Figure 8. For each pair of types, a type for $C_{i,i+1}$ and a type for $C_{j,j+1}$, we can check without difficulty if they are *compatible* by utilizing the fact that (i) in $C_{i+2,j-1}$, where $i+2 \leq j-1$, the number of *pseudo*-terminals, that is, the number of the end vertices of the path segments, of P_1 as well as those of P_2 should be even, (ii) when the subgraph induced by $C_{i+2,j-1}$ is embedded on a rectangle, the pseudo-terminals can be paired up so that the simple continuous curves joining two pseudo-terminals either of P_1 or of P_2 should be pairwise non-intersecting, and (iii) the above mentioned (i) and (ii) also apply to $C_{j+2,n-1} \cup C_{0,i-1}$ (as well as for $C_{i+2,j-1}$). For example, the pair $(X1, X1)$ is incompatible since $C_{i+2,j-1}$ contains three pseudo-terminals, v^0_{i+2}, v^0_{j-1}, and v^2_{j-1}, of P_1 and one pseudo-terminal, v^2_{i+2}, of P_2. The pair $(X1, Z2)$ is also incompatible since the continuous curve joining two pseudo-terminals, v^0_{i+2} and v^2_{j-1}, of P_1 intersects with the curve joining two pseudo-terminals, v^2_{i+2} and v^0_{j-1}, of P_2.

As a result, there remain only four pairs, $(X1, Z1)$, $(Z1, X1)$, $(X2, Z2)$, and $(Z2, X2)$, for

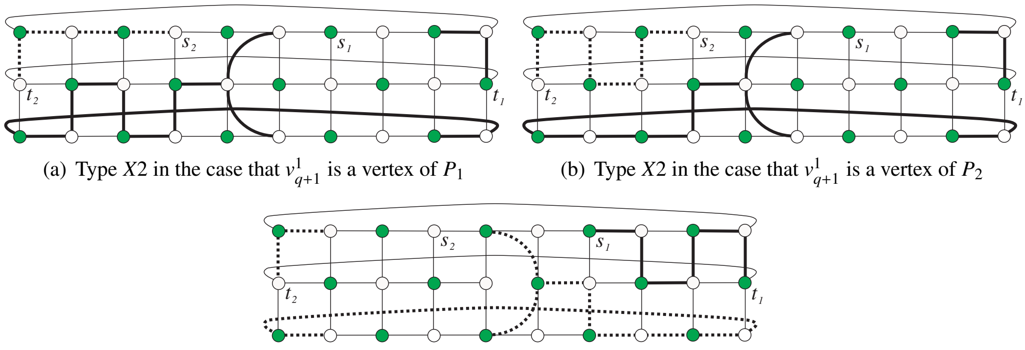

(a) Type $X2$ in the case that v^1_{q+1} is a vertex of P_1 (b) Type $X2$ in the case that v^1_{q+1} is a vertex of P_2

(c) Type $Z1$ in the case that v^1_{j-1} is a vertex of P_1

Figure 10: Illustrations for the proof of Lemma 6. For the configuration (C3), any two disjoint s_1–t_1 and s_2–t_2 paths cannot cover all the vertices of the graph.

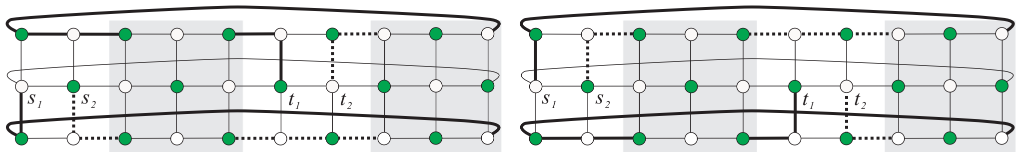

(a) Type $X1$ for $C_{i,i+1}$ and type $Z1$ for $C_{j,j+1}$ (b) Type $X2$ for $C_{i,i+1}$ and type $Z2$ for $C_{j,j+1}$

Figure 11: More illustrations for the proof of Lemma 6. For the configuration (D3), any two disjoint s_1–t_1 and s_2–t_2 paths cannot cover all the vertices of the graph.

which the covering property of the 2-DPC is applied to derive a contradiction. Consider the pair $(X1, Z1)$ shown in Figure 11a. For P_1 and P_2 altogether to cover every vertex of the graph, the subgraph induced by $C_{i+2,j-1}$ should have a paired 2-DPC composed of a v^0_{i+2}–v^0_{j-1} path and a v^2_{i+2}–v^2_{j-1} path. However, this is impossible since all the four pseudo-terminals have the same color, say green, and the induced subgraph has only one more green vertex than white ones. A similar argument holds for the remaining three pairs, $(Z1, X1)$, $(X2, Z2)$, and $(Z2, X2)$. (For the pairs $(Z1, X1)$ and $(Z2, X2)$, the induced subgraph has no paired 2-DPC composed of a v^0_{i+2}–v^2_{i+2} path and a v^0_{j-1}–v^2_{j-1} path.) This completes the entire proof. □

It is interesting to see that, if we relax some conditions exposed on (C3) or (D3), it is possible to construct a paired 2-DPC joining given S and T as shown in the following two Remarks, which will actually be used in the proof of Theorem 5.

Remark 1 (Relaxed (C3)). If the partial conditions $q = j + 1$ and $(n - 1 - p) + i \geq 2$ in the specification of (C3) in Lemma 6 are relaxed so that $q \geq j + 3$ or $(n - 1 - p) + i = 0$, then there exists a paired 2-DPC joining S and T. To prove this, assume w.l.o.g. $i = 0$, i.e., $s_1 = v^0_0$. Suppose $q \geq j + 3$ first. As shown in Figure 12a, it suffices to let P_1 be a Hamiltonian s_1–t_1 path in the subgraph $G^{0,j+1}$ induced by $C_{0,j+1}$ and let $P_2 = (P_a, P_b)$ where P_a is a Hamiltonian s_2–v^2_{q+1} path in $G^{q+1,n-1}$ and P_b is a Hamiltonian v^2_q–t_2 path in $G^{j+2,q}$. Suppose $(n-1-p)+i = 0$ (and $q = j+1$)

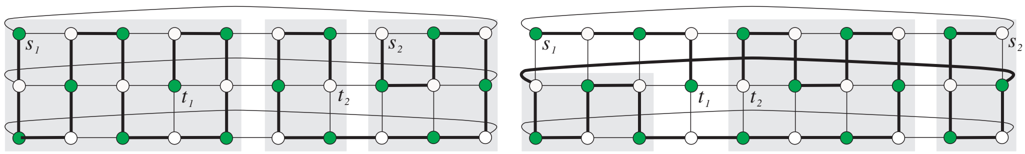

(a) $q \geq j + 3$ (b) $(n - 1 - p) + i = 0$

Figure 12: Paired 2-DPCs for the relaxed configuration (C3).

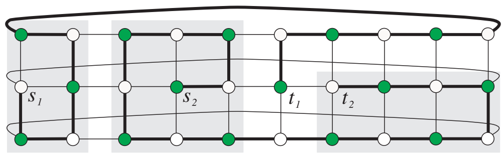

Figure 13: A paired 2-DPC for the relaxed configuration (D3).

now, i.e., $s_2 = v^0_{n-1}$ (see Figure 12b). Then, $C_{1,j-1} \neq \emptyset$ or $C_{q+1,n-2} \neq \emptyset$ since $n \geq 6$. Assume w.l.o.g. the latter holds true. Then, $P_1 = (s_1 = v^0_0, v^0_1, \ldots, v^0_j, v^1_j = t_1)$ and $P_2 = (P_a, P_b, v^2_j, P_c)$ where P_a is a Hamiltonian s_2–v^1_{n-1} path in $G^{n-2,n-1}$, P_b is a Hamiltonian v^1_0–v^2_{j-1} path in $G^{0,j-1}_{1,2}$, and P_c is a Hamiltonian v^2_{j+1}–t_2 path in $G^{j+1,n-3}$. Thus, the claim is proved.

Remark 2 (Relaxed (D3)). If the partial conditions $p = i + 1$ and $q = j + 1$ in the specification of (D3) in Lemma 6 are relaxed so that $p \geq i + 3$ or $q \geq j + 3$, then there exists a paired 2-DPC joining S and T. To prove this, assume w.l.o.g. $p \geq i + 3$ and further assume $i = 0$ so that $s_1 = v^1_0$. As shown in Figure 13, it suffices to let $P_1 = (P_a, v^0_{n-1}, \ldots, v^0_j, v^1_j)$ where P_a is a Hamiltonian s_1–v^0_0 path in the induced subgraph $G^{0,1}$, and let $P_2 = (P_b, v^2_j, P_c)$ where P_b is a Hamiltonian s_2–v^2_{j-1} path in $G^{2,j-1}$, and P_c is a Hamiltonian v^2_{j+1}–t_2 path in $G^{j+1,n-1}_{1,2}$. The claim is also proved.

Now, the next lemma handles the other two inadmissible configurations, (E3) and (F3), regarding to the $3 \times n$ cylindrical grids with even $n \geq 6$ (refer to Figure 14). For its proof, we borrow the notion of the winding number of a closed curve, routinely used in algebraic topology, and extend it to an open curve with orientation. *The winding number of a closed curve* in the plane around a given point measures how many times the curve travels counterclockwise around the point. It depends on the orientation of the curve, and is negative if the curve travels clockwise around the point. In our work, *the winding number of an open curve with orientation* is defined in the same way, but the winding number is allowed to have any real number unlike that of a closed curve that may only be an integer number. For example, if an open curve circles a given point one and half times clockwise, and then circles the point once counterclockwise, then the winding number of the curve will be $-\frac{1}{2}$.

Lemma 7. *For even $n \geq 6$, no $3 \times n$ cylindrical grid G has a paired 2-DPC joining $S = \{s_1, s_2\}$ and $T = \{t_1, t_2\}$ if S and T form any of the following configurations:*

(E3) *$s_1 = v^0_i$, $s_2 = v^0_p$, $t_2 = v^2_q$, $t_1 = v^2_j$, and $c(s_1) = c(s_2) \neq c(t_1) = c(t_2)$ for some i, j, p, and q such that $i < p < q < j$, $q - p - 1 \geq 2$, and $(n - 1 - j) + i \geq 2$; and*

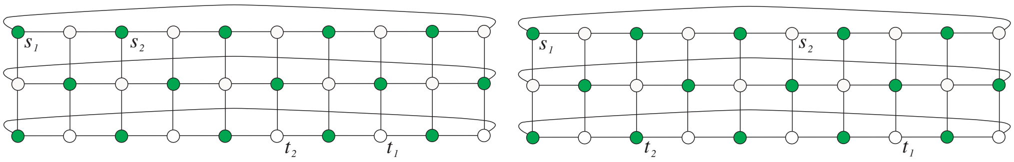

(a) Configuration (E3) (b) Configuration (F3)

Figure 14: Examples of two additional inadmissible configurations for $3 \times n$ cylindrical grids with even $n \geq 6$ (continued from Figure 6).

(F3) *$s_1 = v^0_i$, $t_2 = v^2_q$, $s_2 = v^0_p$, $t_1 = v^2_j$, and $c(s_1) = c(t_2) \neq c(s_2) = c(t_1)$ for some i, j, p, and q such that $q' < j'$, $j' - q' - 1 \geq 2$, and $(n - 1 - p') + i' \geq 2$, where $i' = \min\{i, q\}$, $q' = \max\{i, q\}$, $j' = \min\{j, p\}$, and $p' = \max\{j, p\}$.*

Proof. Suppose to the contrary that there exists a paired 2-DPC composed of an s_1–t_1 path P_1 and an s_2–t_2 path P_2. For the first part of the proof, let the terminals form the configuration (E3). Assume the $3 \times n$ cylindrical grid is embedded on an annulus, where s_1 and s_2 are located on the innermost circle while t_1 and t_2 are located on the outermost circle. Furthermore, we assume that the cocenter of the two circles is the origin of an x, y-plane, s_1 and s_2 respectively are on the positive x and y axes, and t_2 and t_1 respectively are on the negative x and y axes.

If the winding number of P_1 with respect to the origin is $\frac{3}{4}$, where P_1 is assumed to be oriented from s_1 to t_1, then there is no choice but in the subgraph induced by $C_{p,q}$, row 1 is a segment of P_1 whereas rows 0 and 2 are segments of P_2, as shown in Figure 15a. This is because there are only three tracks, i.e. three rows in the subgraph. In the subgraph induced by $(C_{q,n-1} \cup C_{0,p}) \setminus \{s_2, t_2\}$ shown in Figure 15b, moreover, there should exist a paired 3-DPC composed of a v^1_q–t_1 path, a v^0_q–v^2_p path, and an s_1–v^1_p path. We will show, however, that this is impossible. Similar to Claim 2 in the proof of Lemma 6, we can deduce that (v^0_{q+1}, v^0_{q+2}), (v^0_{q+3}, v^0_{q+4}), . . ., (v^0_{j-1}, v^0_j) are edges of the v^0_q–v^2_p path whereas (v^2_{q+1}, v^2_{q+2}), (v^2_{q+3}, v^2_{q+4}), . . ., (v^2_{j-1}, v^2_j) are edges of the v^1_q–t_1 path. Then, (v^0_j, v^1_j) and (v^1_j, v^1_{j+1}) should be edges of the v^0_q–v^2_p path. It follows that both v^0_{j+1} and v^2_{j+1} should be contained in the v^0_q–v^2_p path, which is certainly impossible. (Note that the number, $(n-1-j)+i$, of columns in $C_{j+1,n-1} \cup C_{0,i-1}$ is at least two.) Therefore, the winding number of P_1 cannot be $\frac{3}{4}$.

Similarly, we can prove that the winding number of P_1 cannot be $-\frac{5}{4}$ (under the condition of $q - p - 1 \geq 2$). Figures 15c and 15d illustrate the case when the winding number is $-\frac{5}{4}$. One can immediately observe the symmetry between this case and the case of the winding number being $\frac{3}{4}$. In addition, the winding number cannot be greater than $\frac{3}{4}$; suppose otherwise, we would need more than three tracks in the subgraph induced by $C_{p,q}$. Similarly, the winding number cannot be less than $-\frac{5}{4}$.

Now, there remains only one case where the winding number of P_1 is $-\frac{1}{4}$ as shown in Figure 16a. Since $C_{i+1,p-1}$ is nonempty, P_1 or P_2, say P_1, has a 'U-turn', i.e. a path segment (u, P'_1, v) where $u, v \in C_{r-1}$ and P'_1 is a path of two or three vertices of C_r for some r. Suppose for the first subcase that P_1 has a *wide* U-turn in which P'_1 is a three-vertex path. It follows that $r < p$; suppose otherwise, the subpath between s_1 and v^0_r would separate s_2 and t_2, as shown in Figure 16b, so that P_2 would intersect with P_1, a contradiction. Then, P_1 passes through every vertex of $C_{i,r}$ while P_2 passes through every vertex of $C_{r+1,p}$, where either $C_{i,r}$ or $C_{r+1,p}$ but not both has an

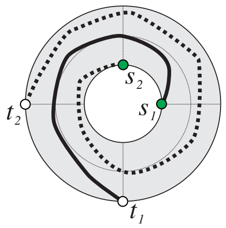

(a) $\omega(P_1) = \frac{3}{4}$

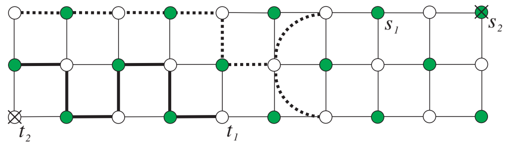

(b) The induced subgraph by $(C_{q,n-1} \cup C_{0,p}) \setminus \{s_2, t_2\}$

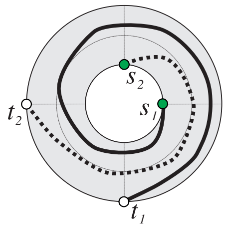

(c) $\omega(P_1) = -\frac{5}{4}$

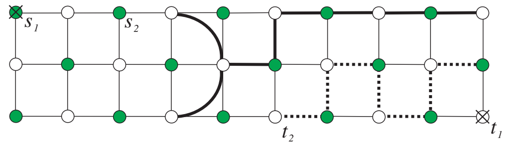

(d) The induced subgraph by $C_{i,j} \setminus \{s_1, t_1\}$.

Figure 15: Embedding of P_1 and P_2 for the configuration (E3) in the case that the winding number of P_1, denoted by $\omega(P_1)$, is $\frac{3}{4}$ or $-\frac{5}{4}$.

even number of columns. If $C_{i,r}$ has an even number of columns, then there are an even number of vertices in $C_{i,r}$ and thus the s_1–v_i^1 subpath of P_1 forms a Hamiltonian path of $C_{i,r}$, as shown in Figure 16c. Note that in C_i, there exists a unique vertex, v_i^1, that has a different color from s_1. It follows that P_1 should advance to v_{i-1}^1 and then pass through both v_{i-1}^0 and v_{i-1}^2, which is a contradiction. If $C_{r+1,p}$ has an even number of columns, then P_2 would advance to v_{p+1}^1 and then pass through both v_{p+1}^0 and v_{p+1}^2, which is also a contradiction. (Note that v_{i-1}^0, v_{i-1}^2, v_{p+1}^0, and v_{p+1}^2 are all nonterminals because $(n-1-j)+i \geq 2$ and $q-p-1 \geq 2$.)

Suppose for the second subcase that P_1 has a *sharp* U-turn in which P_1' is a two-vertex path. We claim $r \geq p$. Suppose $r < p$. Let $z \in C_r$ be the vertex not contained in $V(P_1')$. It follows that if $z = v_r^0$, then $(v_{r-1}^0, v_r^0, v_{r+1}^0)$ should be a path segment of P_1 or of P_2 as shown in Figure 16d, which is impossible; if $z = v_r^2$, then $(v_{r-1}^2, v_r^2, v_{r+1}^2)$ should be a path segment of P_1 or of P_2, which is also impossible. The claim is proved. Now, we have $r \geq p$. As shown in Figures 16e and 16f, P_2 starting at s_2 advances to s_{p+1}^0. Thus P_1 has two disjoint path segments, s_1–v_p^1 path and v_p^2–v_i^1 path, that cover every vertex of $C_{i,p} \setminus s_2$ (since the subgraph induced by the vertex subset is balanced). Then, P_1 has no choice but advances to v_{i-1}^1 and should pass through both nonterminals v_{i-1}^0 and v_{i-1}^2, which is a contradiction. (Recall the condition of $(n-1-j)+i \geq 2$.) This completes the proof for the configuration (E3).

Now, let the set of terminals form the configuration (F3) for the second part of the proof. We assume that the $3 \times n$ cylindrical grid is embedded on an annulus, where s_1 and s_2 are located on the inner circle while t_1 and t_2 are located on the outer circle. Furthermore, we assume the cocenter of the two circles is the origin of an x, y-plane, the vertices of $C_{i'}$ and of $C_{q'}$ respectively are on the positive x and y axes if $i' \neq q'$, and the vertices of $C_{j'}$ and of $C_{p'}$ respectively are on the negative x and y axes if $j' \neq p'$. It may freely be assumed that if $i' = q'$, the vertices of $C_{i'}$

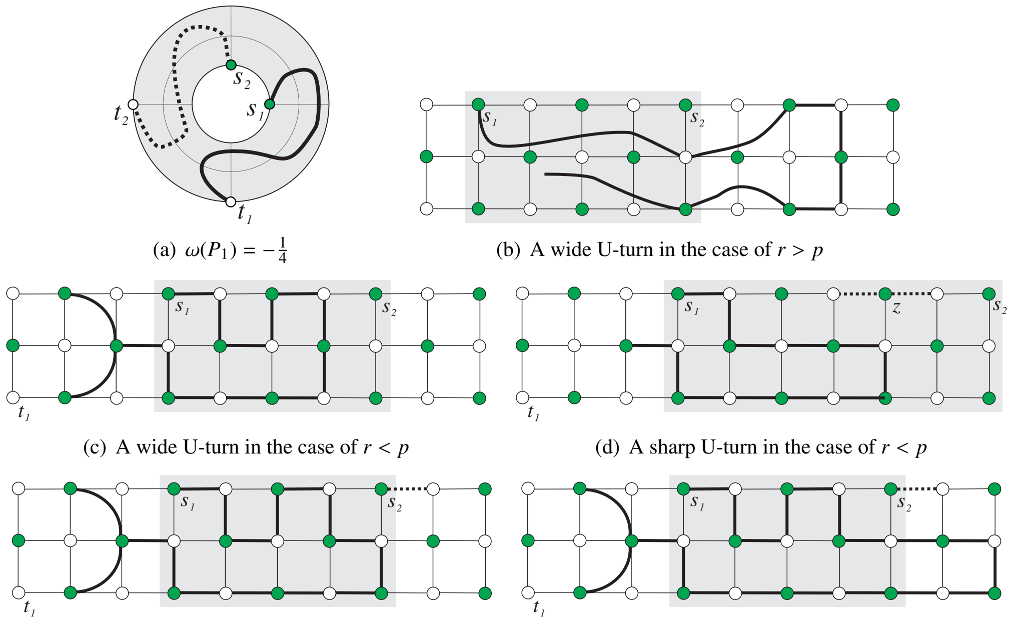

(a) $\omega(P_1) = -\frac{1}{4}$ (b) A wide U-turn in the case of $r > p$

(c) A wide U-turn in the case of $r < p$ (d) A sharp U-turn in the case of $r < p$

(e) A sharp U-turn in the case of $r = p$ (f) A sharp U-turn in the case of $r > p$

Figure 16: Embedding of P_1 and P_2 for the configuration (E3) in the case of $\omega(P_1) = -\frac{1}{4}$.

are either on the positive x axis or on the positive y axis; if $j' = p'$, the vertices of $C_{j'}$ are either on the negative x axis or on the negative y axis.

If the winding number of P_1 with respect to the origin is greater than 1, then the winding number of P_2 is also greater than 1 (see Figure 17a). It follows that $q < i$; suppose $i \leq q$, we would have four or more subpaths (two subpaths of P_1 and two subpaths of P_2), possibly one-vertex paths, between $C_{i'}$ and $C_{q'}$ in the subgraph induced by $C_{i',q'}$, which is clearly impossible since the subgraph has only three rows. Furthermore, the subgraph induced by $C_{i',q'} \setminus \{s_1, t_2\}$ should have a paired 2-DPC composed of a v_q^0–v_i^1 subpath (of P_2) and a v_q^1–v_i^2 subpath (of P_1). This is impossible, however, since the induced subgraph is not balanced but the two pseudo-terminals of each subpath have different colors to each other. Thus, the winding number of P_1 cannot be greater than 1. Symmetrically, we can also prove that the winding number of P_1 cannot be smaller than -1, as illustrated in Figure 17b.

Let the winding number of P_1 be between 0 and 1 exclusive (see Figures 17c and 17d). We consider the subgraph induced by $C_{i',q'}$, where there are two cases whether $q < i$ or $i \leq q$. The case when $q < i$, illustrated in Figure 17e, can be proved in the same way as the proof, illustrated in Figure 16, for the configuration (E3) when the winding number of P_1 is $-\frac{1}{4}$. (In short, P_1 or P_2, say P_2, has a U-turn since $C_{q+1,i-1}$ is nonempty. However, the U-turn can be neither wide nor sharp.) Suppose $i \leq q$ (see Figure 17f). We claim $v_i^2 \in V(P_2)$. Suppose otherwise, v_i^2–t_1 subpath of P_1 would separate s_2 and t_2, a contradiction. Similarly, we have $v_q^0 \in V(P_1)$. It follows that if P_1 passes through some vertex to the left of column i and makes a U-turn, then P_1 visits v_{i-1}^1 and then v_i^1. Similarly, if P_2 passes through some vertex to the right of column q, then P_2 visits v_{q+1}^1

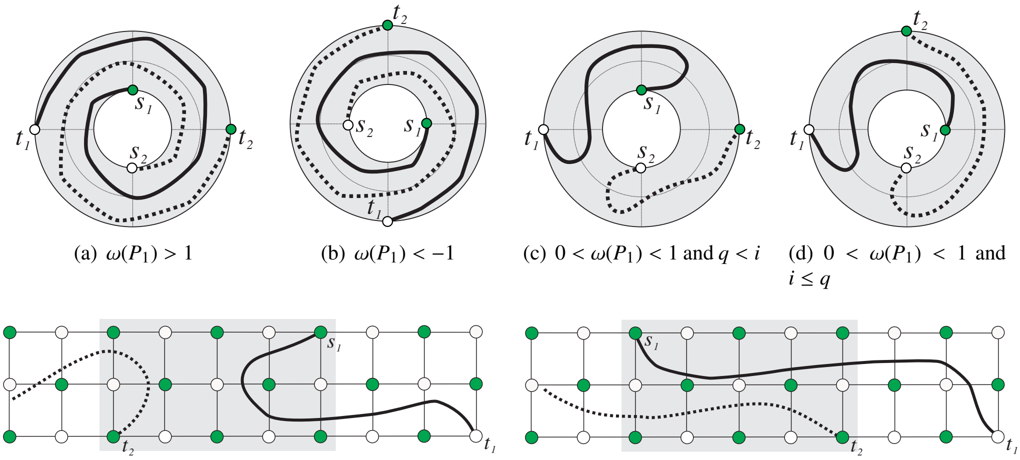

(a) $\omega(P_1) > 1$ (b) $\omega(P_1) < -1$ (c) $0 < \omega(P_1) < 1$ and $q < i$ (d) $0 < \omega(P_1) < 1$ and $i \le q$

(e) The subgraph induced by $C_{i',q'}$ in the case of $q < i$ (f) The subgraph induced by $C_{i',q'}$ in the case of $i \le q$

Figure 17: Embeddings of P_1 and P_2 for the configuration (F3).

and then v_q^1.

From these observations, we can see that if P_1 passes through some vertex to the left of column i, P_1 has two subpaths, the one-vertex subpath (s_1) and the v_i^1–u subpath for some $u \in \{v_q^0, v_q^1\}$, in the subgraph induced by $C_{i,q}$; otherwise, P_1 has a single subpath, s_1–u subpath for some $u \in \{v_q^0, v_q^1\}$, in the induced subgraph. Similarly, P_2 has two subpaths, the one-vertex subpath (t_2) and v_q^1–w subpath, or has a single t_2–w subpath for some $w \in \{v_i^1, v_i^2\}$. The subpath(s) of P_1 and the subpath(s) of P_2 are disjoint paths that altogether cover the induced subgraph.

We claim $u = v_q^1$ or $w = v_i^1$. Suppose otherwise, the subpath(s) of P_1 has one more green vertex than white ones, where $c(s_1)$ and $c(t_2)$ are assumed to be green; the subpath(s) of P_2 also has one more green vertex than white ones. Since the induced subgraph has only one more green vertex than white ones, it is impossible for the subpaths of P_1 and P_2 collectively to cover the induced subgraph. The claim is proved. If P_1 visits v_q^1 and advances to v_{q+1}^1, then there is no choice but P_1 passes through both vertices v_{q+1}^0 and v_{q+1}^2, which is a contradiction. Similarly, if P_2 visits v_i^1 and advances to v_{i-1}^1, then P_2 should pass through both vertices v_{i-1}^0 and v_{i-1}^2, a contradiction. (Note that v_{q+1}^0, v_{q+1}^2, v_{i-1}^0, and v_{i-1}^2 are all nonterminals since $j' - q' - 1 \ge 2$ and $(n - 1 - p') + i' \ge 2$.) The remaining case where $-1 < \omega(P_1) < 0$ is symmetric to the case where $0 < \omega(P_1) < 1$. (Imagine a reflection across the line $y = x$ through the origin.) Therefore, the entire proof is completed. □

As before, some conditions exposed on (E3) or (F3) can be relaxed so that we may construct a paired 2-DPC joining given S and T as shown in the following two Remarks, which will be used in the proof of Theorem 5.

Remark 3 (Relaxed (E3)). If the partial conditions $q - p - 1 \ge 2$ and $(n - 1 - j) + i \ge 2$ in the specification of (E3) in Lemma 7 are relaxed so that $q - p - 1 = 0$ or $(n - 1 - j) + i = 0$, then there exists a paired 2-DPC joining S and T. To prove this, assume w.l.o.g. $q - p - 1 = 0$, i.e., $q = p + 1$, and further assume $i = 0$ so that $s_1 = v_0^0$. As shown in Figure 18, it suffices to let P_1

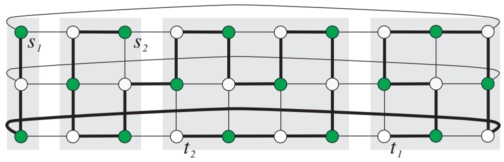

Figure 18: A paired 2-DPC for the relaxed configuration (E3).

be a Hamiltonian s_1–t_1 path in the subgraph induced by $C_0 \cup C_{j,n-1}$ and let $P_2 = (P_a, P_b)$ where P_a is a Hamiltonian s_2–v_p^1 path in $G^{1,p}$ and P_b is a Hamiltonian v_q^1–t_2 path in $G^{q,j-1}$. The claim is proved.

Remark 4 (Relaxed (F3)). If the partial conditions $j' - q' - 1 \geq 2$ and $(n - 1 - p') + i' \geq 2$ in the specification of (F3) in Lemma 7 are relaxed so that $j' - q' - 1 = 0$ or $(n - 1 - p') + i' = 0$, then there exists a paired 2-DPC joining S and T. To prove this, assume w.l.o.g. $j' - q' - 1 = 0$ (i.e., $j' = q' + 1$), $q' - i' \leq p' - j'$, and $i = 0$ ($s_1 = v_0^0$). Suppose $n - 1 - p' \geq 2$ first. If $j \leq p$ (see Figure 19a), then it suffices to let $P_1 = (v_0^0, v_0^1, P_a, P_b, v_p^1, v_p^2, \ldots, v_j^2)$ where P_a is a Hamiltonian v_1^1–v_q^1 path in $G_{0,1}^{1,q}$ and P_b is a Hamiltonian v_j^1–v_{p-1}^1 path in $G_{0,1}^{j,p-1}$, and let $P_2 = (v_p^0, P_c, v_0^2, \ldots, v_q^2)$ where P_c is a Hamiltonian v_{p+1}^0–v_{n-1}^2 path in $G^{p+1,n-1}$. Note that P_a is empty if $q = 0$ and P_b is empty if $j = p$. If $p < j$ (see Figure 19b), then we let $P_1 = (v_0^0, P_a, v_j^2)$ where P_a is a Hamiltonian v_{n-1}^0–v_{j+1}^2 path in $G^{j+1,n-1}$, and let $P_2 = (v_p^0, \ldots, v_j^0, v_j^1, P_b, P_c, v_0^1, v_0^2, \ldots, v_q^2)$ where P_b is a Hamiltonian v_{j-1}^1–v_p^1 path in $G_{1,2}^{p,j-1}$ and P_c is a Hamiltonian v_q^1–v_1^1 path in $G_{0,1}^{1,q}$. Now, suppose $n - 1 - p' = 0$ for the second case. Then, $p' - j' \geq 2$ and $p' = n - 1$. If $j < p$ (see Figure 19c), then we let $P_1 = (P_a, P_b)$ where P_a is a Hamiltonian v_0^0–v_q^1 path in $G_{0,1}^{0,q}$ and P_b is a Hamiltonian v_j^1–v_j^2 path in $G^{j,n-2}$, and let $P_2 = (v_{n-1}^0, v_{n-1}^1, v_{n-1}^2, v_0^2, \ldots, v_q^2)$. If $p < j$ (see Figure 19d), then we let $P_1 = (v_0^0, v_{n-1}^0, v_{n-1}^1, v_{n-1}^2)$ and $P_2 = (P_a, P_b, v_0^1, v_0^2, \ldots, v_q^2)$ where P_a is a Hamiltonian v_p^0–v_p^1 path in $G^{p,n-2}$ and P_b is a Hamiltonian v_q^1–v_1^1 path in $G_{0,1}^{1,q}$. Therefore, the claim is also proved.

Now, we have the theorem for this subsection.

Theorem 5. *For even $n \geq 6$, a $3 \times n$ cylindrical grid G has a paired 2-DPC joining $S = \{s_1, s_2\}$ and $T = \{t_1, t_2\}$ if and only if $S \cup T$ is balanced, and the four terminals in $S \cup T$ do not form an inadmissible configuration equivalent to (A), (B), (C3), (D3), (E3), or (F3).*

Proof. The necessity part of the proof is immediately due to Theorem 1 and Lemmas 6 and 7. On the other hand, the sufficiency part proceeds based on Theorem 4, which reveals the exact condition for the class of the $2 \times n$ cylindrical grids with even $n \geq 6$. (Notice that the subgraph $G_{0,1}$ of a $3 \times n$ cylindrical grid G induced by $R_{0,1}$ is isomorphic to a $2 \times n$ cylindrical grid.) As in the proof of Theorem 3, we assume w.l.o.g. $|R_2 \cap (S \cup T)| \leq |R_0 \cap (S \cup T)|$, from which the following three cases arise with respect to the number of terminals in R_2.

Case 1: *R_2 has no terminal.* If there exists a paired 2-DPC joining S and T in $G_{0,1}$, then it suffices to replace a row-1 edge (u, v) of a path in the 2-DPC with the subpath (u, P_h, v) where P_h is a Hamiltonian path of G_2 that connects the two neighbors of u and v in R_2. Thus hereafter in the

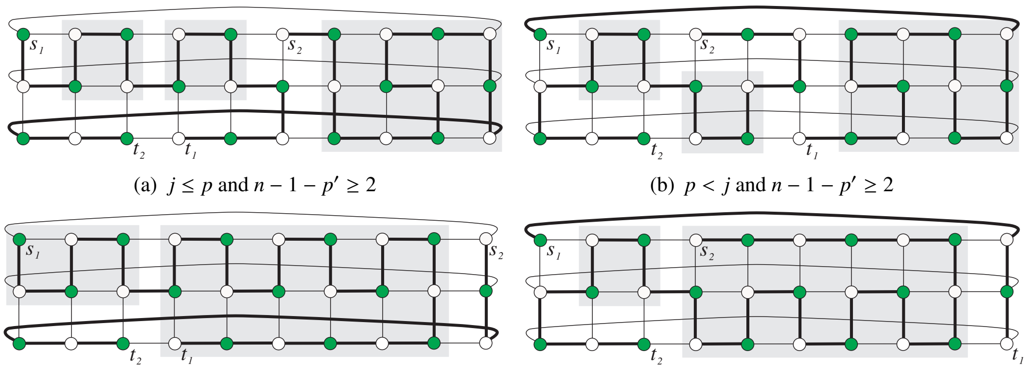

(a) $j \leq p$ and $n-1-p' \geq 2$

(b) $p < j$ and $n-1-p' \geq 2$

(c) $j < p$ and $n-1-p' = 0$

(d) $p < j$ and $n-1-p' = 0$

Figure 19: Paired 2-DPCs for the relaxed configuration (F3).

proof of Case 1, we assume that no such paired 2-DPC exists, i.e., S and T form an inadmissible configuration equivalent to (A), (B2), (C2), or (D2) in $G_{0,1}$.

Suppose for the first subcase that S and T form a configuration equivalent to (A) in $G_{0,1}$. Then, $S \cup T \subset R_1$ because, if otherwise, i.e., $S \cup T \subset R_0$, they would form a configuration equivalent to (A) in G, violating the hypothesis of our theorem. Now, assume w.l.o.g. that $s_1 = v_i^1$, $s_2 = v_p^1$, $t_1 = v_j^1$, and $t_2 = v_q^1$ for some $i < p < j < q$. If $c(s_1) = c(t_2)$ ($\neq c(t_1) = c(s_2)$), then S and T form a configuration equivalent to the relaxed (D3) of Remark 2 and admit a paired 2-DPC (or they would form a configuration equivalent to (D3) in G). If $c(s_1) = c(s_2)$, then S and T also form a configuration equivalent to the relaxed (D3). (Under the assumption that $i = 0$, swap s_2 and t_2 and then consider the automorphism ϕ such that $\phi(v_0^a) = v_0^a$ and $\phi(v_b^a) = v_{n-b}^a$ for $a \in \{0, 1, 2\}$ and $b \in \{1, \ldots, n-1\}$.) Finally, let $c(s_1) = c(t_1) \neq c(s_2) = c(t_2)$. Then, at least one of (s_1, s_2), (s_2, t_1), (t_1, t_2), and (t_2, s_1) is not an edge of G since $n \geq 6$. Let $(s_1, s_2) \notin E(G)$, i.e., $p \geq i + 3$, and further assume $i = 0$. Similar to the construction in Remark 2, it suffices to define $P_1 = (P_a, v_{n-1}^0, \ldots, v_j^0, v_j^1)$ where P_a is a Hamiltonian s_1–v_0^1 path in the induced subgraph $G^{0,1}$, and $P_2 = (P_b, v_j^2, P_c)$ where P_b is a Hamiltonian s_2–v_{j-1}^2 path in $G^{2,j-1}$, and P_c is a Hamiltonian v_{j+1}^2–t_2 path in the subgraph $G_{1,2}^{j+1,n-1}$ induced by $R_{1,2} \cap C_{j+1,n-1}$.

Suppose for the second subcase that S and T form a configuration equivalent to (B2) in $G_{0,1}$. Then, $S \cup T = \{v_i^0, v_i^1, v_j^0, v_j^1\}$ and $c(s_1) = c(t_1) \neq c(s_2) = c(t_2)$ for some i and j with $i \neq j$. Assume w.l.o.g. $i = 0$, $j \leq n/2$, and $s_1 = v_0^0$. Then, it should be that $j \neq 1$ because, if otherwise, S and T would form a configuration equivalent to (B) in G. If $t_1 = v_j^1$ (j odd), then it suffices to define $P_1 = (v_0^0, P_a, v_j^2, v_j^1)$ where P_a is a Hamiltonian v_1^0–v_{j-1}^2 path in $G^{1,j-1}$ and $P_2 = (v_0^1, v_0^2, P_b, v_j^0)$ where P_b is a Hamiltonian v_{n-1}^2–v_{j+1}^0 path in $G^{j+1,n-1}$. If $t_1 = v_j^0$ (j even), then it suffices to define $P_1 = (v_0^0, \ldots, v_j^0)$ and $P_2 = (v_0^1, v_0^2, P_x, P_y)$ where P_x is a Hamiltonian v_{n-1}^2–v_{j+1}^2 path in $G^{j+1,n-1}$ and P_y is a Hamiltonian v_j^2–v_j^1 path in $G_{1,2}^{1,j}$. Suppose for the third subcase that S and T form a configuration equivalent to (C2) in $G_{0,1}$. Assume $s_1 = v_i^0$, $t_1 = v_j^1$, $s_2 = v_p^0$, $t_2 = v_q^1$, and $c(s_1) = c(t_1) \neq c(s_2) = c(t_2)$ for some i, j, p, and q such that $\max\{i, j\} < \min\{p, q\}$. Furthermore, we can assume w.l.o.g. that $i = 0$ and $s_1 = v_0^0$. If $p < q$, then it suffices to find a Hamiltonian s_1–t_1 path in $G^{0,p-1}$ and a Hamiltonian s_2–t_2 path in $G^{p,n-1}$. If $q < p$, then S and T

form a configuration equivalent to the relaxed (C3) of Remark 1 and admit a paired 2-DPC (or they would form a configuration equivalent to (C3) in G). Finally, suppose that S and T form a configuration equivalent to (D2) in $G_{0,1}$. Assume $s_1 = v^0_i$, $s_2 = v^0_p$, $t_1 = v^1_j$, $t_2 = v^1_q$, and $c(s_1) = c(s_2) \neq c(t_1) = c(t_2)$ for some i, j, p, and q such that $i < p < j < q$. Furthermore, we assume w.l.o.g. that $i = 0$ so that $s_1 = v^0_0$. Then, it suffices to define $P_1 = (P_a, P_b)$ where P_a is a Hamiltonian s_1–v^2_{p-1} path in $G^{0,p-1}$ and P_b is a Hamiltonian v^2_p–t_1 path in $G^{p,q-1}_{1,2}$ and $P_2 = (v^0_p, \dots, v^0_{q-1}, P_c)$ where P_c is a Hamiltonian v^0_q–t_2 path in $G^{q,n-1}$.

Case 2: *R_2 has a single terminal.* There exists at least one terminal in R_0 by our assumption that $|R_2 \cap (S \cup T)| \leq |R_0 \cap (S \cup T)|$. The terminal of R_2, say t_2, has two neighbors x_1 and x_2 in R_2, which respectively have unique neighbors y_1 and y_2 in R_1. At least one of y_1 and y_2, say y_1, is a nonterminal since $c(y_1) = c(y_2) = c(t_2)$. If $G_{0,1}$ has a paired 2-DPC composed of an s_1–t_1 path P_1 and an s_2–y_1 path P_2, then G has a paired 2-DPC $\{P_1, (P_2, P_h)\}$ joining S and T where P_h is a Hamiltonian x_1–t_2 path in G_2. Now, for the remaining proof of Case 2, assume that $G_{0,1}$ have no paired 2-DPC joining S and T' where $T' = \{t_1, t'_2\}$ with $t'_2 = y_1$. Then, S and T' form an inadmissible configuration equivalent to (B2), (C2), or (D2) in $G_{0,1}$, from which we find that $|R_0 \cap (S \cup T)| = 2$ and $|R_1 \cap (S \cup T)| = 1$. (Notice that they cannot form a configuration equivalent to (A).) There are two cases up to symmetry: $R_0 \cap (S \cup T) = \{s_1, t_1\}$ and $R_0 \cap (S \cup T) = \{s_1, s_2\}$.

First, let $R_0 \cap (S \cup T) = \{s_1, t_1\}$. Then, S and T' form a configuration equivalent to (B2) where $\{s_1, t_1\} = \{v^0_i, v^0_j\}$ for some i, j and $c(s_1) = c(t_1) \neq c(s_2) = c(t'_2)$. If the vertex y_2 is a nonterminal, then S and $\{t_1, y_2\}$ do not form an inadmissible configuration in $G_{0,1}$ and thus $G_{0,1}$ has a paired 2-DPC composed of s_1–t_1 path and s_2–y_2 path. From this 2-DPC of $G_{0,1}$, a paired 2-DPC of G can be constructed as before. If y_2 is a terminal, then y_2 must be s_2. A paired 2-DPC of G can then be obtained by combining a Hamiltonian s_1–t_1 path of $G_{0,1} \setminus s_2$, which exists by Lemma 2, and the s_2–t_2 path (s_2, P_h) where P_h is a Hamiltonian x_2–t_2 path in G_2.

Secondly, let $R_0 \cap (S \cup T) = \{s_1, s_2\}$. Assume w.l.o.g. $s_1 = v^0_0$ and $s_2 = v^0_p$ for some $p \leq n/2$, and let $t_1 = v^1_j$. We let $P_1 = (v^0_0, \dots, v^0_{p-1})$ and $P_2 = (v^0_p, \dots, v^0_{n-1})$ if $j \notin \{p-1, n-1\}$, and $P_1 = (v^0_0, v^0_{n-1}, v^0_{n-2}, \dots, v^0_{p+1})$ and $P_2 = (v^0_p, v^0_{p-1}, \dots, v^0_1)$ otherwise. Then, $V(P_1) \cup V(P_2) = R_0$ and moreover $(u_1, t_1), (u_2, t_1) \notin E(G)$, where u_i is the sink of P_i (i.e., P_i is an s_i–u_i path) for $i \in \{1, 2\}$. (This is because v^0_1, v^0_{p-1}, v^0_{p+1}, and v^0_{n-1} are all distinct for $p \neq 2$; for $p = 2$, we have $1 = p - 1 < p + 1 < n - 1$ but $j \neq 1$ due to the assumption that $S \cup T$ is balanced.) For the neighbor s'_1 of u_1 in R_1 and the neighbor s'_2 of u_2 in R_1, there exists a paired 2-DPC joining S' and T in $G_{1,2}$ where $S' = \{s'_1, s'_2\}$ since $|R_1 \cap (S' \cup T)| = 3$ and $|R_2 \cap (S' \cup T)| = 1$. (Notice that in no inadmissible configuration of the $2 \times n$ cylindrical grid with even $n \geq 6$, a single row contains an odd number of terminals.) It suffices to merge $\{P_1, P_2\}$ and the 2-DPC of $G_{1,2}$ with edges (u_1, s'_1) and (u_2, s'_2).

Case 3: *R_2 has two terminals.* In this case, R_0 also has two terminals. Suppose $s_1, t_1 \in R_0$ first. Assume w.l.o.g. $s_1 = v^0_0$ and $t_1 = v^0_j$ for some $j \leq n/2$. If $G_{1,2}$ has a paired 2-DPC composed of an s'_1–t'_1 path P_1 and an s_2–t_2 path P_2 where $s'_1 = v^1_{j-1}$ and $t'_1 = v^1_{n-1}$, then G has a paired 2-DPC composed of $(v^0_0, \dots, v^0_{j-1}, P_1, v^0_{n-1}, v^0_{n-2}, \dots, v^0_j)$ and P_2. Otherwise, it follows from Theorem 4 that $c(s'_1) = c(t'_1) \neq c(s_2) = c(t_2)$ and moreover $\{s_2, t_2\} = \{v^2_{j-1}, v^2_{n-1}\}$. Then, a paired 2-DPC of G can be obtained, similar to the subcase $R_0 \cap (S \cup T) = \{s_1, s_2\}$ of Case 2, from a paired 2-DPC of $G_{1,2}$ composed of a v^1_{j+1}–v^1_1 path and an s_2–t_2 path. (Note that $\{v^1_{j+1}, v^1_1\} \neq \{v^1_{j-1}, v^1_{n-1}\}$ for every j since $n \geq 6$.) Thus hereafter in the proof of Case 3, we suppose $s_1, s_2 \in R_0$. Assume w.l.o.g. $s_1 = v^0_0$ and $s_2 = v^0_p$ for some $p \leq n/2$. Similar to the previous subcase, if $G_{1,2}$ has a paired 2-DPC composed of an s'_1–t_1 path P_1 and an s'_2–t_2 path P_2 where $s'_1 = v^1_{p-1}$ and $s'_2 = v^1_{n-1}$, then G

has a paired 2-DPC composed of $(v_0^0, \ldots, v_{p-1}^0, P_1)$ and $(v_p^0, \ldots, v_{n-1}^0, P_2)$. Now, let no such paired 2-DPC of $G_{1,2}$ exist. It follows that S' and T form an inadmissible configuration equivalent to (B2), (C2), or (D2) in $G_{1,2}$, where $S' = \{s_1', s_2'\}$.

First, suppose that S' and T form a configuration equivalent to (B2). Then, $c(s_1') \neq c(s_2')$ and thus p is odd. Furthermore, $t_2 = v_{p-1}^2$ and $t_1 = v_{n-1}^2$. Observe that S and T form a configuration equivalent to the relaxed (F3) of Remark 4. Thus, there exists a paired 2-DPC joining S and T. Second, suppose that S' and T form a configuration equivalent to (C2). Similar to the previous subcase, $c(s_1') \neq c(s_2')$ and p is odd. Furthermore, $c(s_1') = c(t_1)$ and $c(s_2') = c(t_2)$. If we let $t_1 = v_j^2$ and $t_2 = v_q^2$, then j is odd and q is even, so that $c(s_1) = c(t_2) \neq c(t_1) = c(s_2)$. There are four possibilities on the locations of t_1 and t_2 (subject to the condition that S' and T form a configuration equivalent to (C2)): (i) $p \leq j < q < n-1$, (ii) $p \leq j < n-1$ & $0 \leq q < p-1$, (iii) $0 \leq q < j < p-1$, and (iv) $0 < j < p-1$ & $p < q < n-1$. For the possibility (i), S and T form a configuration equivalent to (F3) if $p-1 \geq 2$ & $q-j-1 \geq 2$; otherwise, they form a configuration equivalent to the relaxed (F3) of Remark 4 and admit a paired 2-DPC. Similar to (i), we can derive that for each of the remaining three possibilities, S and T form a configuration equivalent to (F3), or form a configuration equivalent to the relaxed (F3) and admit a paired 2-DPC. Finally, suppose that S' and T form a configuration equivalent to (D2). Then, $c(s_1') = c(s_2')$ and thus p is even. If we let $t_1 = v_j^2$ and $t_2 = v_q^2$, then j and q are both odd, so that $c(s_1) = c(s_2) \neq c(t_1) = c(t_2)$. There are two possibilities on the locations of t_1 and t_2: (i) $0 < j < q < p-1$ and (ii) $p < q < j < n-1$. For the possibility (i), S and T form a configuration equivalent to (E3) if $j \geq 3$; otherwise, they form a configuration equivalent to the relaxed (E3) and admit a paired 2-DPC. Also for the possibility (ii), S and T form a configuration equivalent to (E3) (when $q-p-1 \geq 2$), or form a configuration equivalent to the relaxed (E3) and admit a paired 2-DPC. This completes the proof. □

Corollary 4. *For even $n \geq 6$, a $3 \times n$ cylindrical grid G has an unpaired 2-DPC joining $S = \{s_1, s_2\}$ and $T = \{t_1, t_2\}$ if and only if $S \cup T$ is balanced.*

Proof. This corollary follows from Theorem 5, which immediately allows to deduce that G has a paired 2-DPC composed of s_1–t_1 and s_2–t_2 paths, or has a paired 2-DPC composed of s_1–t_2 and s_2–t_1 paths. □

3.5. 2-DPCs in $m \times n$ cylindrical grids with $m = 4$ and even $n \geq 6$

In this section, we finally provide the proof for the base step ($m = 4$) of Theorem 2, where Theorems 4 and 5 are used for two smaller dimensions of cylindrical grids, i.e., $2 \times n$ and $3 \times n$.

Theorem 6. *For even $n \geq 6$, a $4 \times n$ cylindrical grid G has a paired 2-DPC joining $S = \{s_1, s_2\}$ and $T = \{t_1, t_2\}$ if and only if $S \cup T$ is balanced, and the four terminals in $S \cup T$ do not form an inadmissible configuration equivalent to (A), (B), or (C).*

Proof. The necessity part is due to Theorem 1. For the sufficiency part, throughout the proof, we assume w.l.o.g. that either (i) $|R_3 \cap (S \cup T)| < |R_0 \cap (S \cup T)|$, or (ii) $|R_3 \cap (S \cup T)| = |R_0 \cap (S \cup T)|$ and $|R_2 \cap (S \cup T)| \leq |R_1 \cap (S \cup T)|$. Now, we construct the wanted 2-DPC paths P_1 and P_2, respectively joining s_1 & t_1, and s_2 & t_2, for each of the following three cases.

Case 1: *R_3 has no terminal.* If $G_{0,2}$ has a paired 2-DPC joining S and T, then it suffices to replace an arbitrary row-2 edge (u, v) of a path in the 2-DPC with the subpath (u, P_h, v), where P_h is the Hamiltonian path of G_3, connecting the two neighbors of u and v in R_3. If there

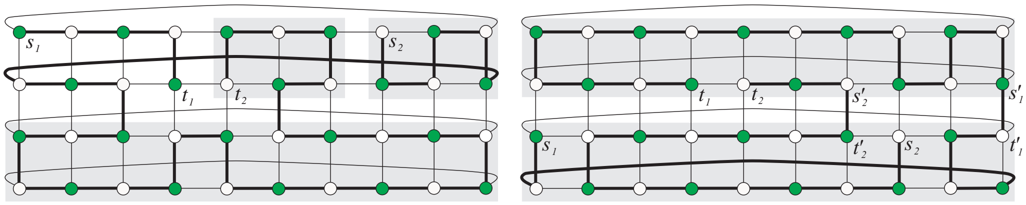

(a) $R_0 \cap (S \cup T) \neq \emptyset$ (b) $R_0 \cap (S \cup T) = \emptyset$

Figure 20: Illustrations for the proof of Theorem 6: S and T form an inadmissible configuration (C3) in $G_{0,2}$.

exists no such 2-DPC, S and T must form an inadmissible configuration in $G_{0,2}$, which may be equivalent to (A), (B), (C3), (D3), (E3), or (F3) by Theorem 5. First, the configuration (A) is not possible. Otherwise, the two troublesome cases of $S \cup T \subset R_0$ and $S \cup T \subset R_2$ would lead us to the contradictions that the terminal sets also form an inadmissible configuration in G, and they violate the assumption (ii), respectively. Second, the same is true for the configuration (B) because, otherwise, the same configuration would also be found in G. Then, the remaining cases are that $G_{0,2}$ suffers from an inadmissible configuration equivalent to (C3), (D3), (E3), or (F3).

First, consider the configuration equivalent to (C3) in $G_{0,2}$, in which either $R_0 \cap (S \cup T) \neq \emptyset$ (see Figure 20a) or $R_0 \cap (S \cup T) = \emptyset$ (see Figure 20b). If $R_0 \cap (S \cup T) \neq \emptyset$, assume w.l.o.g. that $s_1 = v^0_0$, $t_1 = v^1_j$, $t_2 = v^1_q$, and $s_2 = v^0_p$ for some j, p, and q such that $0 < j < q < p$, $q = j + 1$, $n - 1 - p \geq 2$, and $c(s_1) = c(t_1) \neq c(s_2) = c(t_2)$, where at least one of $C_{1,j-1}$ and $C_{q+1,p-1}$ is nonempty because, otherwise, S and T would form the inadmissible configuration (C) in G. When $C_{q+1,p-1} \neq \emptyset$ (the case of $C_{1,j-1} \neq \emptyset$ is handled similarly), we can build a wanted 2-DPC such that $P_1 = (v^0_0, v^0_1, \ldots, v^0_j, v^1_j)$ and $P_2 = (P_a, v^1_0, v^1_1, \ldots, v^1_{j-1}, P_h, P_b)$ where P_a is a Hamiltonian s_2–v^1_{n-1} path in $G^{p,n-1}_{0,1}$, P_h is a Hamiltonian v^2_{j-1}–v^2_{q+1} path in $G_{2,3}$, and P_b is a Hamiltonian v^1_{q+1}–t_2 path in $G^{q,p-1}_{0,1}$. If $R_0 \cap (S \cup T) = \emptyset$, assume w.l.o.g. that $s_1 = v^2_0$, $t_1 = v^1_j$, $t_2 = v^1_q$, and $s_2 = v^2_p$ for some j, p, andP_b is a Hamiltonian v^1_{q+1}–t_2 path in $G^{q,p-1}_{0,1}$ q such that $0 < j < q < p$, $q = j+1$, $n-1-p \geq 2$, and $c(s_1) = c(t_1) \neq c(s_2) = c(t_2)$. Let $s'_1 = v^1_{n-1}$, $t'_1 = v^2_{n-1}$, $s'_2 = v^1_{p-1}$, and $t'_2 = v^2_{p-1}$. If $p - 1 \neq q$, then, by Theorem 4, $G_{0,1}$ has a paired 2-DPC composed of an s'_1–t_1 path and an s'_2–t_2 path. Also, $G_{2,3}$ trivially has a paired 2-DPC composed of an s_1–t'_1 path and an s_2–t'_2 path. Then, it suffices to merge the two DPCs with edges (s'_1, t'_1) and (s'_2, t'_2). If $p - 1 = q$, then $s'_2 = t_2$ and there exists a Hamiltonian s'_1–t_1 path P_h in $G_{0,1} \setminus t_2$. The Hamiltonian path P_h and one-vertex path (t_2) are disjoint and cover the vertices of $G_{0,1}$. Thus, it is sufficient to merge the two and the paired 2-DPC of $G_{2,3}$.

Second, consider the configuration equivalent to (D3) in $G_{0,2}$, where we assume w.l.o.g. that $s_1 = v^1_0$, $s_2 = v^1_1$, $t_1 = v^1_j$, and $t_2 = v^1_q$ for some j and q such that $1 < j < q$, $q = j + 1$, and $c(s_1) = c(t_2) \neq c(t_1) = c(s_2)$ as illustrated in Figure 21a. Then, we have $P_1 = (v^1_0, v^0_0, \ldots, v^0_j, v^1_j)$ and $P_2 = (v^1_1, \ldots, v^1_{j-1}, P_h, P_a)$ where P_h is a Hamiltonian v^2_{j-1}–v^2_{q+1} path in $G_{2,3}$ and P_a is a Hamiltonian v^1_{q+1}–t_2 path in $G^{q,n-1}_{0,1}$. Third, consider the configuration equivalent to (E3) in $G_{0,2}$, where we assume w.l.o.g. that $s_1 = v^0_0$, $s_2 = v^0_p$, $t_2 = v^2_q$, and $t_1 = v^2_j$ for some j, p, and q such that $0 < p < q < j$, $q - p - 1 \geq 2$, $n - 1 - j \geq 2$, and $c(s_1) = c(s_2) \neq c(t_1) = c(t_2)$ as illustrated in Figure 21b. If we let $s'_1 = v^1_{p-1}$ and $s'_2 = v^1_{n-1}$, then $\{s'_1, s'_2\}$ and T does not form an inadmissible configuration in $G_{1,3}$ (note that $c(s'_1) = c(s'_2)$, $\{s'_1, s'_2\} \subset R_1$, and $T \subset R_2$), implying the existence

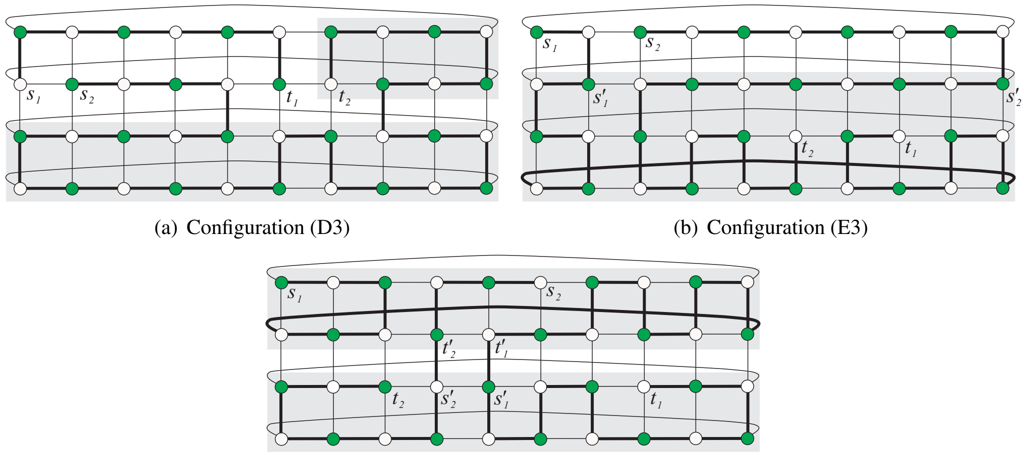

(a) Configuration (D3)

(b) Configuration (E3)

(c) Configuration (F3)

Figure 21: Illustrations for the proof of Theorem 6: S and T form an inadmissible configuration in $G_{0,2}$.

of a paired 2-DPC of $G_{1,3}$, composed of an s'_1–t_1 path P'_1 and an s'_2–t_2 path P'_2. From this, we can construct a paired 2-DPC of G: $P_1 = (v^0_0, \ldots, v^0_{p-1}, P'_1)$ and $P_2 = (v^0_p, \ldots, v^0_{n-1}, P'_2)$. Finally, consider the configuration equivalent to (F3) in $G_{0,2}$, where we assume w.l.o.g. that $s_1 = v^0_0$, $t_2 = v^2_q$, $s_2 = v^0_p$, and $t_1 = v^2_j$ for some j, p, and q such that $q < j'$, $j' - q - 1 \geq 2$, $n - 1 - p' \geq 2$, and $c(s_1) = c(t_2) \neq c(s_2) = c(t_1)$, where $j' = \min\{j, p\}$ and $p' = \max\{j, p\}$ (as illustrated in Figure 21c). For $t'_2 = v^1_{q+1}$ and $t'_1 = v^1_{q+2}$, $G_{0,1}$ has a paired 2-DPC composed of an s_1–t'_1 path and an s_2–t'_2 path by Theorem 4. Also for $s'_2 = v^2_{q+1}$ and $s'_1 = v^2_{q+2}$, $G_{2,3}$ has a paired 2-DPC composed of an s'_1–t_1 path and an s'_2–t_2 path. It suffices to merge the two DPCs with edges (s'_1, t'_1) and (s'_2, t'_2).

Case 2: *R_3 has a single terminal.* Let the terminal in R_3 be, say, t_2. Then, at least one of the two neighbors in R_2 of the two neighbors in R_3 of t_2 is a nonterminal (otherwise, $S \cup T$ would be unbalanced). Let t'_2 be such a nonterminal in R_2, and x be the common neighbor in R_3 of t'_2 and t_2. If $G_{0,2}$ has a paired 2-DPC composed of an s_1–t_1 path P_1 and an s_2–t'_2 path P'_2, then we have a wanted 2-DPC of G, $\{P_1, (P'_2, P_h)\}$, where P_h is a Hamiltonian x–t_2 path of G_3. Suppose that no such paired 2-DPC of $G_{0,2}$ exists, meaning S and $\{t_1, t'_2\}$ form an inadmissible configuration in $G_{0,2}$. From the fact that R_0 has at least one terminal by the assumption (i) and (ii), and any four terminals forming an inadmissible configuration equivalent to (A), (B), (C3), or (D3) occupy at most two consecutive rows, it must be that S and $\{t_1, t'_2\}$ form an inadmissible configuration equivalent to (E3) or (F3) in $G_{0,2}$, for which we can see that $s_1 = v^0_0$ w.l.o.g. and $s_2 = v^0_p$ for some $p > 0$, both in R_0, and $t_1 \in R_2$. If we let $s'_1 = v^1_{p-1}$ and $s'_2 = v^1_{n-1}$, we can find a paired 2-DPC in $G_{1,3}$ composed of an s'_1–t_1 path P''_1 and an s'_2–t_2 path P''_2 since no inadmissible configuration possible for a $3 \times n$ cylindrical grid has a single terminal in a row. Thus, there exists a paired 2-DPC of G composed of $(v^0_0, \ldots, v^0_{p-1}, P''_1)$ and $(v^0_p, \ldots, v^0_{n-1}, P''_2)$.

Case 3: *R_3 has two terminals.* First, suppose $s_2 := v^3_p$ and $t_2 := v^3_q$ (for some p and q) are the two terminals in R_3. If we let $s'_2 = v^2_{q-1}$ and $t'_2 = v^2_{p-1}$, there exists a paired 2-DPC in $G_{0,2}$ composed of an s_1–t_1 path P_1 and an s'_2–t'_2 path P'_2 (since $s_1, t_1 \in R_0$ by the assumption (i) and

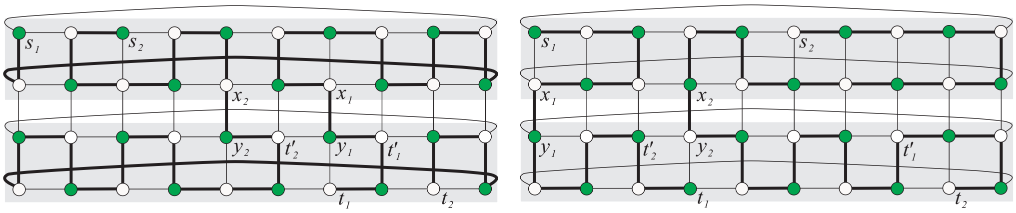

(a) Configuration (E3) (b) Configuration (F3)

Figure 22: Illustrations for the proof of Theorem 6: S and $\{t'_1, t'_2\}$ form an inadmissible configuration in $G_{0,2}$.

$s'_2, t'_2 \in R_2$). Thus, G has a desired paired 2-DPC $\{P_1, P_2\}$, where P_2 is the concatenation of $(v^3_p, v^3_{p+1}, \dots, v^3_{q-1})$, P'_2, and $(v^3_{p-1}, v^3_{p-2}, \dots, v^3_q)$. Second, suppose $t_1 := v^3_j$ and $t_2 := v^3_q$ (for some j and q) are the two terminals in R_3. If we let $t'_1 = v^2_{q-1}$ and $t'_2 = v^2_{j-1}$, there exists a paired 2-DPC in $G_{0,2}$ composed of an s_1–t'_1 path P'_1 and an s_2–t'_2 path P'_2 unless S and $\{t'_1, t'_2\}$ form an inadmissible configuration equivalent to (E3) or (F3) in $G_{0,2}$. If such a 2-DPC exists in $G_{0,2}$, then we have a wanted 2-DPC of G: $P_1 = (P'_1, v^3_{q-1}, v^3_{q-2}, \dots, v^3_j)$ and $P_2 = (P'_2, v^3_{j-1}, v^3_{j-2}, \dots, v^3_q)$.

Now, we are left with two subcases: Suppose that S and $\{t'_1, t'_2\}$ form a configuration equivalent to (E3) in $G_{0,2}$, in which we assume w.l.o.g. that $s_1 = v^0_0$, $s_2 = v^0_p$, $t'_2 = v^2_{j-1}$, and $t'_1 = v^2_{q-1}$ for some p, j, and q such that $0 < p < j-1 < q-1$, $(j-1)-p-1 \geq 2$, $n-1-(q-1) \geq 2$, and $c(s_1) = c(s_2) \neq c(t'_1) = c(t'_2)$ (thus $t_1 = v^3_j$ and $t_2 = v^3_q$ as illustrated in Figure 22a). If we let $x_1 = t^1_j$, $x_2 = t^1_{j-2}$, $y_1 = t^2_j$, and $y_2 = t^2_{j-2}$, then by Theorem 4, $G_{0,1}$ has a paired 2-DPC composed of an s_1–x_1 path and an s_2–x_2 path, and $G_{2,3}$ has a paired 2-DPC composed of a y_1–t_1 path and a y_2–t_2 path (note that the assumed configuration enforces that y_2 and t_2 must belong to different columns). Then, we can find a wanted 2-DPC of G by merging the two DPCs through edges (x_1, y_1) and (x_2, y_2). For the second subcase, suppose that S and $\{t'_1, t'_2\}$ form a configuration equivalent to (F3) in $G_{0,2}$, in which we assume w.l.o.g. that $s_1 = v^0_0$, $s_2 = v^0_p$, $t'_1 = v^2_{q-1}$, and $t'_2 = v^2_{j-1}$ for some p, j, and q such that $j-1 < \min\{p, q-1\}$, $\min\{p, q-1\}-(j-1)-1 \geq 2$, $n-1-\max\{p, q-1\} \geq 2$, and $c(s_1) = c(t'_2) \neq c(s_2) = c(t'_1)$ (thus $t_1 = v^3_j$ and $t_2 = v^3_q$ as illustrated in Figure 22b). If we let $x_1 = v^1_0$, $x_2 = v^1_j$, $y_1 = v^2_0$, and $y_2 = v^2_j$, then by Theorem 4, $G_{0,1}$ has a paired 2-DPC composed of an s_1–x_1 path and an s_2–x_2 path, and $G_{2,3}$ has a paired 2-DPC composed of a y_1–t_1 path and a y_2–t_2 path (note that the assumed configuration enforces that x_2 and s_2 (and y_1 and t_2 also) must belong to different columns). Then, we can find a wanted 2-DPC of G by merging the two DPCs through edges (x_1, y_1) and (x_2, y_2). This completes the entire proof. □

4. Two-disjoint path covers in toroidal grids

As stated in Lemma 3, an $m \times n$ toroidal grid with $m, n \geq 4$, both even, always has a paired 2-DPC if and only if the set of four terminals is balanced. An interesting further question is whether it is also true even when there is a single faulty edge in the graph. From the foundings with respect to the cylindrical grids, we can show that the fact also holds for such faulty toroidal grids.

Theorem 7. *For an $m \times n$ toroidal grid G with $m, n \geq 4$, both even, and an arbitrary edge e_f of G, $G \setminus e_f$ has a paired 2-DPC joining $S = \{s_1, s_2\}$ and $T = \{t_1, t_2\}$ if and only if $S \cup T$ is balanced.*

Proof. The necessity part is obvious since $G \setminus e_f$ is a balanced bipartite graph. To prove sufficiency, assume that $S \cup T$ is balanced, and, w.l.o.g., e_f is a column edge between the zeroth and the $(m-1)$th row. Consider the spanning subgraph H obtained by removing all the column edges, including e_f, between the zeroth and the $(m-1)$th row, which is now isomorphic to an $m \times n$ cylindrical grid. If H has a paired 2-DPC joining S and T, so does $G \setminus e_f$ and we are done. Suppose otherwise. Then, S and T form an inadmissible configuration equivalent to either (A), (B), (C), (A1), or (C1) in H. Note that, by Theorems 2 and 3, and the fact that (A) and (C) are special cases of (A1) and (C1), respectively, (A), (B), and (C) may arise for $n \geq 4$ whereas (A1) and (C1) arise only for $n = 4$.

Case 1: *S and T form a configuration equivalent to (A).* Let $s_1 = v_i^0$, $s_2 = v_p^0$, $t_1 = v_j^0$, and $t_2 = v_q^0$ for some $i < p < j < q$ (see Figure 23a). There are four disjoint paths in G_0 that altogether cover the vertices of G_0: the s_1–v_{p-1}^0 path, the s_2–v_{j-1}^0 path, the v_{q-1}^0–t_1 path, and the v_{i-1}^0–t_2 path. If e_f is not a column-$(i-1)$ edge, let $s_1' = v_{p-1}^1$, $s_2' = v_{j-1}^1$, $t_1' = v_{q-1}^1$, and $t_2' = v_{i-1}^{m-1}$, for which there exists a paired 2-DPC joining $\{s_1', s_2'\}$ and $\{t_1', t_2'\}$ in $G_{1,m-1}$ because the inadmissible configurations specified by Theorems 2, 3, and 5, may not contain an odd number of terminal(s) in a row as in the current terminal sets. Then, we can build a wanted 2-DPC of $G \setminus e_f$ by connecting the s_1–v_{p-1}^0 path and the v_{q-1}^0–t_1 path using the s_1'–t_1' path, and the s_2–v_{j-1}^0 path and the v_{i-1}^0–t_2 path using the s_2'–t_2' path. If e_f is a column-$(i-1)$ edge, then a desired 2-DPC of $G \setminus e_f$ can be constructed similarly except that we let $t_1' = v_{q-1}^{m-1}$ and $t_2' = v_{i-1}^1$, and use $(v_{q-1}^{m-1}, v_{q-1}^0)$ as a wrap-around edge.

Case 2: *S and T form a configuration equivalent to (B).* Assume w.l.o.g. that $s_1 = v_0^r$, $t_1 = v_1^{r+1}$, $s_2 = v_1^r$, and $t_2 = v_0^{r+1}$ for some $r < m-2$ (see Figure 23b). Consider, first, that $r \geq 1$, in which we select an arbitrary wrap-around edge (x_1, y_1), other than e_f, with $x_1 \in R_0$ and $y_1 \in R_{m-1}$, and another edge (x_2, y_2) from the column 2 or 3 such that $x_2 \in R_r$, $y_2 \in R_{r+1}$, and $c(x_2) \neq c(x_1)$. Then, $G_{0,r}$ has a paired 2-DPC composed of an s_1–x_1 path and an s_2–x_2 path for the reason stated in the preceding case. Similarly, $G_{r+1,m-1}$ has a paired 2-DPC composed of a y_1–t_1 path and a y_2–t_2 path. Merging the two DPCs with edges (x_1, y_1) and (x_2, y_2) leads to a desired 2-DPC of $G \setminus e_f$. Second, let $r = 0$. If e_f is not incident with s_1, let $s_1' = v_0^{m-1}$ and $s_2' = v_{n-1}^1$, for which we can find a paired 2-DPC of $G_{1,m-1}$ composed of an s_1'–t_1 path and an s_2'–t_2 path. Then, we can build a paired 2-DPC of $G \setminus e_f$ by connecting s_1 with the s_1'–t_1 path, and the path $(v_1^0, \ldots, v_{n-1}^0)$ with the s_2'–t_2 path. If e_f is incident with s_1, a wanted 2-DPC can be constructed similarly except that we let $s_1' = v_2^1$ and $s_2' = v_1^{m-1}$, and use (v_1^{m-1}, v_1^0) as a wrap-around edge.

Case 3: *S and T form a configuration equivalent to (C).* Assume w.l.o.g. that $s_1 = v_0^0$, $t_1 = v_1^1$, $t_2 = v_2^1$, and $s_2 = v_3^0$ (see Figure 23c). First, when e_f is not incident with v_1^0, we have a paired 2-DPC of $G \setminus e_f$, where the s_1–t_1 path is (s_1, v_0^1, t_1) and the s_2–t_2 path is the concatenation of a Hamiltonian s_2–v_3^1 path of $G_{0,1}^{3,n-1}$, a Hamiltonian v_3^2–v_1^{m-1} path of $G_{2,m-1}$, and the path (v_1^0, v_2^0, t_2). Second, when e_f is incident with v_1^0, the desired s_1–t_1 path is (s_1, v_1^0, t_1) and the s_2–t_2 path is the concatenation of a Hamiltonian s_2–v_{n-1}^1 path of $G_{0,1}^{3,n-1}$, the vertex v_0^1, a Hamiltonian v_0^2–v_2^{m-1} path of $G_{2,m-1}$, and finally the path (v_2^0, t_2).

Case 4: *S and T form a configuration equivalent to (A1).* First of all, recall that $n = 4$ in this case. Now, assume w.l.o.g. that $s_1, t_1 \in R_{r_1}$, $s_2, t_2 \in R_{r_2}$, and $c(s_1) = c(t_1) \neq c(s_2) = c(t_2)$ for

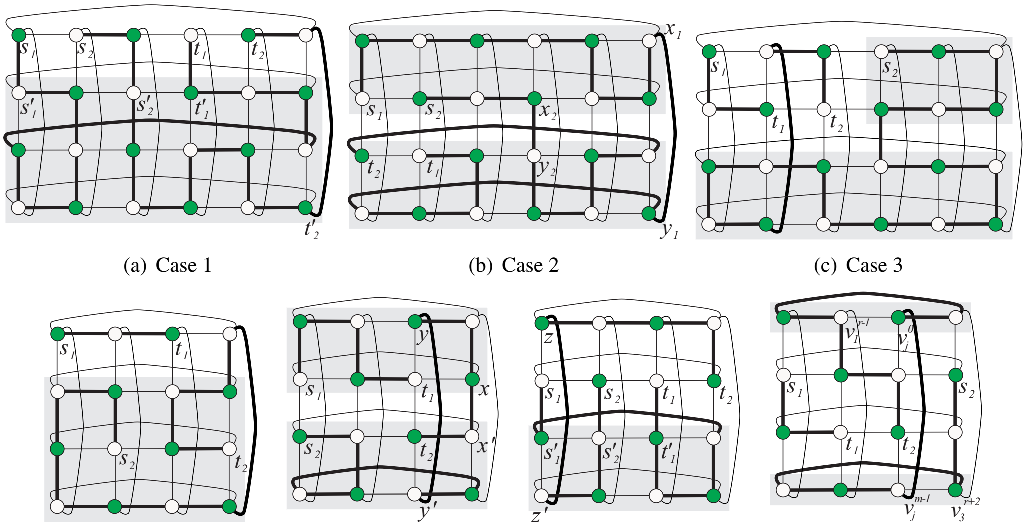

(a) Case 1 (b) Case 2 (c) Case 3

(d) Case 4: $0 = r_1 < r_2$ (e) Case 4: $0 < r_1 < r_2$ (f) Case 4: $0 < r_1 = r_2$ (g) Case 5

Figure 23: Illustrations for the proof of Theorem 7: S and T form an inadmissible configuration in the spanning cylindrical grid.

some r_1 and r_2 such that $r_1 \leq r_2$ and $r_1 \leq m-1-r_2$ (see Figures 23d through 23f). Consider, first, that $r_1 < r_2$. If $r_1 = 0$, assume further w.l.o.g. that $s_1 = v_0^0$ and $t_1 = v_2^0$. Then, by Corollary 2, there is an unpaired 2-DPC of $G_{1,m-1}$ joining the balanced terminal sets $\{s_2, t_2\}$ and $\{v_3^1, v_3^{m-1}\}$. If the column edge e_f is not incident with v_3^0, we have a desired 2-DPC of $G \setminus e_f$, where the s_1–t_1 path is (s_1, v_1^0, t_1) and the s_2–t_2 path is the concatenation of the two disjoint paths in the unpaired 2-DPC via v_3^0. If e_f is incident with v_3^0, we can build a wanted 2-DPC of $G \setminus e_f$ similarly with (s_1, v_3^0, t_1) and the concatenation of the pair of an unpaired 2-DPC paths of $G_{1,m-1}$, joining $\{s_2, t_2\}$ and $\{v_1^1, v_1^{m-1}\}$ via v_1^0. If $r_1 \neq 0$ (and thus $r_2 \neq m-1$), then we select two vertices $x \in R_{r_1}$ and $y \in R_0$ such that $c(x) = c(y) \neq c(s_1) = c(t_1)$, and moreover e_f is not incident with y, for which we can find a paired 2-DPC in G_{0,r_1} composed of an s_1–t_1 path and an x–y path (note the r_1th row contains three terminals for G_{0,r_1}). Furthermore, if we let x' be the neighbor of x in R_{r_1+1}, and y' the neighbor of y in R_{m-1}, we can also find an unpaired 2-DPC of $G_{r_1+1,m-1}$ joining the balanced terminal sets $\{s_2, t_2\}$ and $\{x', y'\}$. Then, the s_1–t_1 path and the proper concatenation of the remaining three paths form a desired 2-DPC of $G \setminus e_f$. Second, let $r_1 = r_2$. If $r (:= r_1) = 0$, then S and T form an inadmissible configuration equivalent to (A), leading us to Case 1. So, let $r \neq 0$ (and thus $r \neq m-1$ too), in which it is further assumed w.l.o.g. that $s_1 = v_0^r$, $s_2 = v_1^r$, $t_1 = v_2^r$, and $t_2 = v_3^r$. For a vertex $z \in R_0$ chosen in such a way that $c(z) = c(t_2)$ and z is not incident with e_f, consider first a Hamiltonian z–v_3^{r-1} path, P_h, in $G_{0,r-1}$. Also, for $s_1' := v_0^{r+1}$, $s_2' := v_1^{r+1}$, $t_1' := v_2^{r+1}$, and the neighbor z' of z in R_{m-1}, $G_{r+1,m-1}$ has a paired 2-DPC composed of an s_1'–t_1' path, P_1, and an s_2'–z' path, P_2. Then, we have a paired 2-DPC $\{(s_1, P_1, t_1), (s_2, P_2, P_h, t_2)\}$ of $G \setminus e_f$.

Case 5: *S and T form a configuration equivalent to (C1).* Again, $n = 4$ in this case. Assume w.l.o.g. that $s_1 = v_0^r$, $t_1 = v_1^{r+1}$, $t_2 = v_2^{r+1}$, and $s_2 = v_3^r$ for some r (see Figure 23g). First, if $r = 0$ or $m-2$, S and T form an inadmissible configuration equivalent to (C), leading to Case 3 (note that when $r = m-2$, an automorphism mapping v^i_j to v^i_{j+2} for $i \in \{0,\dots,m-1\}$ and $j \in \{0,\dots,n-1\}$ will easily lead to such an equivalence). Next, assume $1 \le r \le m-3$. Given e_f, there is always a vertex v^0_j with $c(v^0_j) = c(s_2)$ which is not incident with e_f. Then, there are a Hamiltonian v^{r+2}_3–v^{m-1}_j path, P_h, in $G_{r+2,m-1}$ and a Hamiltonian v^0_j–v^{r-1}_1 path, P'_h in $G_{0,r-1}$. From these, we can build a wanted 2-DPC of $G \setminus e_f$, where the s_1–t_1 path is (s_1, v^{r+1}_0, t_1) and the s_2–t_2 path is $(s_2, v^{r+1}_3, P_h, P'_h, v^r_1, v^r_2, t_2)$. This completes our proof. □

A natural extension of Theorem 7 would be to allow more fault edges, but a counterexample against it is found easily. For example, for $e_f = (v^0_1, v^1_1)$ and $e'_f = (v^1_0, v^1_1)$, $G\setminus\{e_f, e'_f\}$ has no paired 2-DPC joining $S = \{s_1, s_2\}$ and $T = \{t_1, t_2\}$ such that $s_1 = v^1_2$, $s_2 = v^2_1$, $c(s_1) = c(s_2) \ne c(t_1) = c(t_2)$, and $t_1, t_2 \ne v^1_1$. In fact, there even exists no unpaired 2-DPC joining these terminals. Finally, we should mention that the paired 2-DPC problem was studied in [24] for a single-vertex-faulted bipartite toroidal grid $G \setminus v_f$, in which it was shown that $G \setminus v_f$ has a paired 2-DPC if and only if one of the four terminals has the same color as v_f and the other three have the other color.

Acknowledgement

This research was supported by Basic Science Research Program through the National Research Foundation of Korea (NRF) funded by the Ministry of Education, Science and Technology (Grant Nos. 2012R1A1A2005511 and 2012R1A1A2008958).

References

[1] E.M. Arkin, S.P. Fekete, K. Islam, H. Meijer, J.S.B. Mitchell, Y. Núñez-Rodríguez, V. Polishchuk, D. Rappaport, and H. Xiao, "Not being (super)thin or solid is hard: A study of grid Hamiltonicity," *Computational Geometry* **42(6-7)**, pp. 582–605, 2009.

[2] K. Asdre and S.D. Nikolopoulos, "The 1-fixed-endpoint path cover problem is polynomial on interval graphs," *Algorithmica* **58(3)**, pp. 679–710, 2010.

[3] J.A. Bondy and U.S.R. Murty, *Graph Theory*, 2nd printing, Springer, 2008.

[4] R. Caha and V. Koubek, "Hamiltonian cycles and paths with a prescribed set of edges in hypercubes and dense sets," *J. Graph Theory* **51(2)**, pp. 137–169, 2006.

[5] X.-B. Chen, "Many-to-many disjoint paths in faulty hypercubes," *Inf. Sci.* **179(18)**, pp. 3110–3115, 2009.

[6] X.-B. Chen, "Paired many-to-many disjoint path covers of hypercubes with faulty edges," *Inf. Process. Lett.* **112(3)**, pp. 61–66, 2012.

[7] X.-B. Chen, "Paired many-to-many disjoint path covers of the hypercubes," *Inf. Sci.* **236**, pp. 218–223, 2013.

[8] C.C. Chen and N.F. Quimpo, "On strongly Hamiltonian abelian group graphs," in *Proc. Australian Conference on Combinatorial Mathematics (Lecture Notes in Mathematics #884)*, pp. 23–34, 1980.

[9] J. Chvátalová, "Optimal labelling of a product of two paths," *Discrete Math.* **11(3)**, pp. 249–253, 1975.

[10] M. Desjarlais and R. Molina, "Counting spanning trees in grid graphs," *Congressus Numerantium* **145**, pp. 177–185, 2000.

[11] T. Dvořák and P. Gregor, "Hamiltonian paths with prescribed edges in hypercubes," *Discrete Math.* **307**, pp. 1982–1998, 2007.

[12] T. Dvořák and P. Gregor, "Partitions of faulty hypercubes into paths with prescribed endvertices," *SIAM J. Disc. Math.* **22(4)**, pp. 1448–1461, 2008.

[13] J. Ellis and R. Warren, "Lower bounds on the pathwidth of some grid-like graphs," *Discrete Appl. Math.* **156(5)**, pp. 545–555, 2008.

[14] M.J. Golin, Y.-C. Leung, Y. Wang, and X. Yong, "Counting structures in grid graphs, cylinders and tori using transfer matrices: survey and new results," in *Proc. Workshop on Analytic Algorithmics and Combinatorics*, Vancouver, Canada, Jan. 2005.

[15] V.S. Gordon, Y.L. Orlovich, and F. Werner, "Hamiltonian properties of triangular grid graphs," *Discrete Math.* **308(24)**, pp. 6166–6188, 2008.

[16] P. Gregor and T. Dvořák, "Path partitions of hypercubes," *Inform. Proc. Lett.* **108(6)**, pp. 402–406, 2008.

[17] A. Itai, C.H. Papadimitriou, and J.L. Szwarcfiters, "Hamilton paths in grid graphs," *SIAM J. Comput.* **11(4)**, pp. 676–686, 1982.

[18] S. Jo, J.-H. Park, and K.Y. Chwa, "Paired 2-disjoint path covers and strongly Hamiltonian laceability of bipartite hypercube-like graphs," *Inf. Sci.* **242**, pp. 103–112, 2013.

[19] S. Jo, J.-H. Park, and K.Y. Chwa, "Paired many-to-many disjoint path covers in faulty hypercubes," *Theoretical Computer Science* **513**, pp. 1–24, Nov. 2013.

[20] V. Junnila, "New lower bound for 2-identifying code in the square grid," *Discrete Appl. Math.* **161(1314)**, pp. 2042–2051, 2013.

[21] S.-Y. Kim, J.-H. Lee, and J.-H. Park "Disjoint path covers in recursive circulants $G(2^m,4)$ with faulty elements," *Theor. Comp. Sci.* **412(35)**, pp. 4636–4649, 2011.

[22] S.-Y. Kim and J.-H. Park, "Paired many-to-many disjoint path covers in recursive circulants $G(2^m,4)$," *IEEE Trans. Computers* **62(12)**, pp. 2468–2475, Dec. 2013.

[23] H.-C. Kim and J.-H. Park, "Fault Hamiltonicity of two-dimensional torus networks," in *Proc. Workshop on Algorithms and Computation (WAAC 2000)*, Tokyo, Japan, pp. 110–117, July 2000.

[24] H.-D. Kim and J.-H. Park, "Many-to-many disjoint path covers in two-dimensional bipartite tori with a single vertex fault," *Journal of KIISE* **39(5)**, pp. 333–342, Oct. 2012.

[25] P.-L. Lai and H.-C. Hsu, "The two-equal-disjoint path cover problem of matching composition network," *Inf. Process. Lett.* **107(1)**, pp. 18–23, 2008.

[26] T. Laihonen, "On robust identification in the square and king grids," *Discrete Appl. Math.* **154(17)**, pp. 2499–2510, 2006.

[27] D. Liu and J. Li, "Many-to-many n-disjoint path covers in n-dimensional hypercubes," *Inf. Process. Lett.* **110(14-15)**, pp. 580–584, 2010.

[28] F. Luccio and C. Mugnia, "Hamiltonian paths on a rectangular chessboard," in *Proc. 16th Annual Allerton Conf.*, pp. 161–173, 1978.

[29] K. Makino, "Toward a polynomial time algorithm for 2-link puzzle," in *Proc. Workshop on Algorithms and Computation (WAAC 2005)*, Seoul, Korea, Aug. 2005.

[30] K. Makino, "2-disjoint path covers in mesh-torus," *Publications of the Research Institute for Mathematical Sciences 1489*, Kyoto University, pp. 181–187, 2006.

[31] J.R. Munkres, *Topology*, 2nd edition, Prentice-Hall, Inc., 2000.

[32] S.C. Ntafos and S.L. Hakimi, "On path cover problems in digraphs and applications to program testing, *IEEE Trans. Software Eng.* **5(5)**, pp. 520–529, Sept. 1979.

[33] J.-H. Park, "Many-to-many disjoint path covers in two-dimensional tori," *Journal of KIISE* **38(1)**, pp. 42–48, Feb. 2011.

[34] J.-H. Park and I. Ihm, "Single-source three-disjoint path covers in cubes of connected graphs," *Inform. Proc. Lett.* **113(14-16)**, pp. 527–532, 2013.

[35] J.-H. Park and I. Ihm, "Disjoint path covers in cubes of connected graphs," *Discrete Math.* **325**, pp. 65–73, 2014.

[36] J.-H. Park and H.-C. Kim, "Fault-Hamiltonicity of product graph of path and cycle," in *Proc. Int'l Computing and Combinatorics Conf. (COCOON 2003)*, Big Sky, MT, pp. 319–328, July 2003.

[37] J.-H. Park, H.-C. Kim, and H.-S. Lim, "Many-to-many disjoint path covers in hypercube-like interconnection networks with faulty elements," *IEEE Trans. Parallel & Distrib. Syst.* **17(3)**, pp. 227–240, Mar. 2006.

[38] J.-H. Park, H.-C. Kim, and H.-S. Lim, "Many-to-many disjoint path covers in the presence of faulty elements," *IEEE Trans. Computers* **58(4)**, pp. 528–540, Apr. 2009.

[39] O. Pikhurko and J. Wojciechowski, "Edge-bandwidth of grids and tori," *Theor. Comp. Sci.* **369(1-3)**, pp. 35–43, 2006.

[40] J. Rolim, O. Sýkora, and I. Vrt'o, "Optimal cutwidths and bisection widths of 2- and 3-dimensional meshes," in *Proc. Workshop on Graph-Theoretic Concepts in Computer Science (WG 1995)*, Aachen, Germany, June 1995.

[41] Y.-K. Shih and S.-S. Kao, "One-to-one disjoint path covers on k-ary n-cubes," *Theor. Comp. Sci.* **412(35)**, pp. 4513–4530, 2011.

[42] G.J. Simmons, "Almost all n-dimensional rectangular lattices are Hamilton-laceable," in *Proc. 9th Southeastern Conf. on Combinatorics, Graph Theory, and Computing*, pp. 649–661, 1978.

[43] C.-H. Tsai, J.M. Tan, Y.-C. Chuang, and L.-H. Hsu, "Fault-free cycles and links in faulty recursive circulant graphs," in *Proc. Workshop on Algorithms and Theory of Computation (ICS 2000)*, pp. 74–77, 2000.

[44] S. Zhang and S. Wang, "Many-to-many disjoint path covers in k-ary n-cubes," *Theor. Comp. Sci.* **491**, pp. 103–118, 2013.

Appendix

Proof of Theorem 3 for the base case of $m = 2$. (It will give a better understanding of this proof if the readers notice that the graph G is isomorphic to the 3-dimensional hypercube.) For the case of $c(s_1) = c(t_1)$, we assume w.l.o.g. that $\{s_1, t_1\} = \{v_0^0, v_2^0\}$ and moreover, $\{s_2, t_2\} = \{v_1^0, v_0^1\}$. Then, we have a paired 2-DPC $\{(v_0^0, v_3^0, v_2^0), (v_1^0, v_1^1, v_2^1, v_3^1, v_0^1)\}$. Now, let $c(s_1) \neq c(t_1)$. Suppose $(s_1, t_1) \in E(G)$ for the first case. We assume w.l.o.g. that $\{s_1, t_1\} = \{v_0^0, v_0^1\}$. If $\{s_2, t_2\} = \{v_2^0, v_2^1\}$, we have a desired 2-DPC $\{(v_0^0, v_1^0, v_1^1, v_0^1), (v_2^0, v_3^0, v_3^1, v_2^1)\}$; Otherwise, we have a 2-DPC $\{P_1, P_2\}$, where $P_1 = (s_1, t_1)$ and P_2 is a Hamiltonian s_2–t_2 path of $G^{1,3}$ obtained by Lemma 1. Suppose $(s_1, t_1) \notin E(G)$ for the second case. We assume w.l.o.g. that $\{s_1, t_1\} = \{v_0^0, v_2^1\}$. We further assume $(s_2, t_2) \notin E(G)$; Suppose otherwise. Then, this case can be reduced to the first one by exchanging $\{s_1, t_1\}$ with $\{s_2, t_2\}$. Then, there remain two possibilities up to symmetry: (i) for $\{s_2, t_2\} = \{v_0^1, v_2^0\}$, we have $\{(v_0^0, v_1^0, v_1^1, v_2^1), (v_0^1, v_3^1, v_3^0, v_2^0)\}$; and (ii) for $\{s_2, t_2\} = \{v_1^1, v_3^0\}$, we have $\{(v_0^0, v_1^0, v_2^0, v_2^1), (v_1^1, v_0^1, v_3^1, v_3^0)\}$. Thus, the base case is verified. □

Proof of Theorem 4 for the base case of $n = 6$. (Note that an inadmissible configuration equivalent to (D2) may not occur for this case of $n = 6$.) We will construct a paired 2-DPC composed of an s_1–t_1 path P_1 and an s_2–t_2 path P_2 in the following two cases:

Case 1: *There exists C_i, say C_0, such that $C_i \subseteq S \cup T$.* If $C_0 = \{s_1, t_1\}$, it suffices to find a Hamiltonian s_1–t_1 path in $G^{0,p-1}$ and a Hamiltonian s_2–t_2 path in $G^{p,5}$ for some p such that $\{s_2, t_2\} \subseteq C_{p,5}$ and $\{s_2, t_2\} \cap C_p \neq \emptyset$. Now, we assume w.l.o.g. $s_1 = v_0^0$, $s_2 = v_0^1$, $t_1 \in C_j$, and $t_2 \in C_q$ for some $j \leq q$. Suppose $j = q$ first. Then, we have $c(s_1) \neq c(t_1)$. (Suppose otherwise. Then, S and T form an inadmissible configuration equivalent to (B2).) If we remove two edges (s_1, s_2) and (t_1, t_2) from a Hamiltonian cycle $(v_0^1, v_0^0, v_1^0, v_1^1, v_2^1, v_2^0, v_3^0, v_3^1, v_4^1, v_4^0, v_5^0, v_5^1, v_0^1)$ of G, there remain desired two paths. Next, suppose $j < q$. If $c(s_1) = c(t_1)$, we have $P_1 = (s_1, P_1')$ and $P_2 = (s_2, P_2')$ for a Hamiltonian v_1^0–t_1 path P_1' of $G^{1,j}$ and a Hamiltonian v_5^1–t_2 path P_2' of $G^{j+1,5}$; Otherwise, there are three subcases: (i) for $t_1 \in R_0$, we have $P_1 = (v_0^0, \ldots, v_j^0)$ and $P_2 = (v_0^1, \ldots, v_j^1, P_2')$, where P_2' is a Hamiltonian v_{j+1}^1–t_2 path of $G^{j+1,5}$; (ii) for $t_2 \in R_1$, we have $P_2 = (v_0^1, v_5^1, \ldots, v_q^1)$ and $P_1 = (v_0^0, v_5^0, \ldots, v_q^0, P_1')$, where P_1' is a Hamiltonian v_{q-1}^0–t_1 path of $G^{1,q-1}$; and (iii) for $t_1 \in R_1$ & $t_2 \in R_0$ (i.e., $t_1 = v_2^1$ & $t_2 = v_4^0$), we have $P_1 = (v_0^0, v_5^0, v_5^1, v_4^1, v_3^1, v_2^1)$ and $P_2 = (v_0^1, v_1^1, v_1^0, v_2^0, v_3^0, v_4^0)$.

Case 2: *$C_i \nsubseteq S \cup T$ for all $i \in \{0, \ldots, 5\}$.* Assume w.l.o.g. $s_1 = v_0^0$, and let $t_1 \in C_j$, $s_2 \in C_p$, and $t_2 \in C_q$ for some distinct indices j, p, and q. There are two subcases up to symmetry: $0 < j < p < q$ and $0 < p < j < q$. Suppose $0 < j < p < q$ first. If $c(s_1) \neq c(t_1)$, it suffices to let P_1 be a Hamiltonian s_1–t_1 path of $G^{0,p-1}$ and P_2 be a Hamiltonian s_2–t_2 path of $G^{p,5}$. Otherwise, we assume w.l.o.g. $t_1 \in \{v_1^1, v_2^0\}$ (because $S \cup T$ would form an inadmissible configuration equivalent to (C2) if $t_1 = v_3^1$). Then, there are two possibilities up to symmetry: (i) for $t_1 = v_1^1$ & $s_2 = v_2^1$ & $t_2 = v_4^1$, we have $P_1 = (v_0^0, v_1^0, v_2^0, v_3^0, v_4^0, v_5^0, v_5^1, v_0^1, v_1^1)$ and $P_2 = (v_2^1, v_3^1, v_4^1)$; and (ii) for $t_1 = v_2^0$ & $s_2 = v_3^0$ & $t_2 = v_5^0$, we have $P_1 = (v_0^0, v_1^0, v_2^0)$ and $P_2 = (v_3^0, v_3^1, v_2^1, v_1^1, v_0^1, v_5^1, v_4^1, v_4^0, v_5^0)$.

Next, suppose $0 < p < j < q$. We assume w.l.o.g. $t_1 \in C_{2,3}$. There are four subcases up to symmetry: (i) for $t_1 = v_2^0$ ($s_2 = v_1^0$ & $t_2 = v_4^1$), we have $P_1 = (v_0^0, v_0^1, v_5^1, v_5^0, v_4^0, v_3^0, v_2^0)$ and $P_2 = (v_1^0, v_1^1, v_2^1, v_3^1, v_4^1)$; (ii) for $t_1 = v_2^1$ & $s_2 = v_1^0$, we have $P_1 = (v_0^0, v_0^1, v_1^1, v_2^1)$ and $P_2 = (v_1^0, v_2^0, P_2')$, where P_2' is a Hamiltonian v_3^0–t_2 path of $G^{3,5}$; (iii) for $t_1 = v_3^0$ & $s_2 = v_1^1$, we have $P_1 = (v_0^0, v_1^0, v_2^0, v_2^1, v_3^1, v_3^0)$ and $P_2 = (v_1^1, v_0^1, P_2')$, where P_2' is a Hamiltonian v_5^1–t_2 path of $G^{4,5}$ (note that supposing $s_2, t_2 \in R_0$ leads to an inadmissible configuration equivalent to (A)); and (iv) for $t_1 = v_3^1$ & $s_2 = v_1^0$, we have $P_1 = (v_0^0, v_0^1, v_1^1, v_2^1, v_3^1)$ and $P_2 = (v_1^0, v_2^0, v_3^0, P_2')$, where P_2' is a Hamiltonian v_4^0–t_2 path of $G^{4,5}$. Therefore, the base case is verified. □